

The Thermal Conductivity, Thermal Diffusivity and Isobaric Heat Capacity of Toluene and Argon

L. Sun,¹ J. E. S. Venart,^{1, 2} and R. C. Prasad³

Received August 28, 2001

This paper presents absolute measurements for the thermal conductivity and thermal diffusivity of toluene obtained with a transient hot-wire instrument employing coated wires over the density interval of 735 to 870 kg·m⁻³. A new expression for the influence of the wire coating is presented, and an examination of the importance of a nonuniform wire radius is verified with measurements on argon from 296 to 323 K at pressures to 61 MPa. Four isotherms were measured in toluene between 296 and 423 K at pressures to 35 MPa. The measurements have an uncertainty of less than $\pm 0.5\%$ for thermal conductivity and $\pm 2\%$ for thermal diffusivity. Isobaric heat capacity results, derived from the measured values of thermal conductivity and thermal diffusivity, using a density determined from an equation of state, have an uncertainty of $\pm 3\%$ after taking into account the uncertainty of the applied equation of state. The measurements demonstrate that isobaric specific heat determinations can be obtained successfully with the transient hot wire technique over a wide range of fluid states provided density values are available.

KEY WORDS: argon; fluid thermal radiation; heat capacity; thermal conductivity; thermal diffusivity; toluene; transient hot wire technique.

1. INTRODUCTION

The transient line source instrument provides rapid and accurate measurements of the fluid thermal conductivity. A series of corrections must be made to account for differences between the actual and ideal heat transfer

¹ Department of Mechanical Engineering, University of New Brunswick, P.O. Box 4400, Fredericton, New Brunswick, E3B 5A3 Canada.

² To whom correspondence should be addressed. E-mail: jvenart@nbnet.nb.ca

³ Department of Engineering, University of New Brunswick, Saint John, New Brunswick, E2L 4L5 Canada.

models. To measure the thermal conductivity of electrically conducting fluids, or those with high polarity, a wire with a layer of electrical insulation has been used to avoid current leakage. The original correction for the influence of the coating was developed by Nagasaka and Nagashima [1]. There have been few attempts to measure the thermal diffusivity of fluids using coated wires, however.

In this work, a new expression that considers the influence of wire coating has been developed and measurements made for the thermal conductivity and thermal diffusivity of liquid toluene. Additional corrections for the influence of fluid thermal radiation [2], nonuniformity of the wire radius, and a systematic zero time temperature bridge offset [2-4] were employed and the results verified with measurements on argon. Measurements of the thermal conductivity and thermal diffusivity of toluene have been made from 296 to 423 K at pressures to 35 MPa and for argon from 296 to 323 K at pressures to 61 MPa. The thermal conductivity data have an estimated uncertainty of less than $\pm 0.5\%$, while the uncertainty for the thermal diffusivity and the derived isobaric heat capacity is estimated at $\pm 3\%$.

2. METHOD

The transient hot-wire method is widely accepted as a primary instrument for accurate measurements of fluid thermal conductivity for a wide variety of fluids. Its use for thermal diffusivity has, however, been limited due to the lack of reproducibility in the results [4]. The ideal working equation for thermal conductivity is based on the transient solution of Fourier's law for an infinite line source [5]. The ideal temperature rise of the fluid at the wire-fluid interface, $r = a$, at time t is

$$\Delta T = \frac{q}{4\pi\lambda(\rho, T)} \ln \frac{4\alpha t}{a^2 C}, \quad (1)$$

where

$$\Delta T = \Delta T_w + \sum \delta T_i, \quad (2)$$

and $\sum \delta T_i$, are appropriate corrections to the measured temperature rise, ΔT_w , and q is the power per unit length to the wire; λ is the thermal conductivity; $\alpha = \lambda / (\rho C_p)$ is the thermal diffusivity; ρ is the density; and C_p is the isobaric heat capacity, all for the fluid, with $C = 1.781 \dots$ the exponential of Euler's constant.

The thermal conductivity is usually determined from the slope of a linear regression of the temperature difference, ΔT , vs. $\ln(t)$ data via Eq. (1) and assigned to a reference temperature, T_r [5]

$$T_r = T_0 + \frac{1}{2} [\Delta T(t_1) + \Delta T(t_2)] \quad (3)$$

since over the measurement period from t_1 to t_2 both λ and C_p vary linearly with respect to temperature. Here $\Delta T(t_1)$ and $\Delta T(t_2)$ represent the temperature rise at the start, t_1 , and end, t_2 , of the measurement.

In instruments using coated wires, an expression that considered the influence of the coating was developed by Nagasaka and Nagashima [1]. In their analysis, however, even when the thickness of the coating is set to zero, the influence of the coating still persists and since the process that produced this equation is not provided in Ref. 1, the reason is not known. For this reason, a new expression for the temperature rise that considers the influence of the thermal properties of the wire, the coating, and the fluid was developed (Appendix A [3]). This new analysis gives

$$\begin{aligned} \Delta T_1(r, t) = & \frac{q}{4\pi\lambda_3} \left[\ln\left(\frac{4\alpha_3 t}{a_2^2 C}\right) + \frac{2\lambda_3}{\lambda_2} \ln\left(\frac{a_2}{a_1}\right) + \frac{a_1^2}{2\lambda_3 t} \left(\frac{\lambda_2}{\alpha_2} - \frac{\lambda_1}{\alpha_1} \right) \ln\left(\frac{4\alpha_3 t}{a_2^2 C}\right) \right. \\ & + \frac{a_2^2}{2\lambda_3 t} \left(\frac{\lambda_3}{\alpha_3} - \frac{\lambda_2}{\alpha_2} \right) \ln\left(\frac{4\alpha_3 t}{a_2^2 C}\right) + \left(\frac{a_1^2}{\alpha_2 t} - \frac{a_1^2}{\alpha_1 t} \right) \ln\left(\frac{a_2}{a_1}\right) \\ & \left. + \frac{1}{2} \left(\frac{a_1^2 - a_2^2}{\alpha_2 t} + \frac{a_2^2}{\alpha_3 t} - \frac{a_1^2}{\alpha_1 t} + \frac{r^2}{2\alpha_1 t} \right) - \frac{\lambda_3(r^2 - a_1^2)}{\lambda_1 a_1^2} \right], \end{aligned} \quad (4)$$

where subscripts 1, 2, and 3 denote the bare wire, coating, and test fluid, respectively; r is the radial position relative to the axis of the wire; and a_1 and a_2 are the radii of the wire core and outer coating layer, respectively. In this expression, when the thickness of the coating goes to zero, the influence of the coating disappears and the expression for the ideal bare wire, Eq. (1), results. Though this result leads to a more accurate correction, its application produces little change in the reported thermal conductivity ($\leq 0.1\%$) relative to those obtained through use of the previous result [1].

To determine the influence of fluid thermal radiation, it is usually necessary to consider the full form of the applicable integral-differential energy equation. The solution of this, however, can not be obtained analytically and a numerical solution was previously used to examine the potential for fluid thermal radiation in a series of the n-alkanes [6]. The correction procedure proposed was computationally intensive and could not easily be applied to routine experimental procedure. Nieto de Castro

and colleagues showed, however, that for some fluids the dominant correction term arises from fluid emission. This consideration permitted a simplified but approximate analytic solution [7–9]. In their analysis, however, the wire had been considered part of the fluid since the inner boundary condition was taken to be $r = 0$. To eliminate this influence and examine its impact, a new solution was obtained using the correct boundary condition, $r = a$, and considering the thermophysical properties of the wire; this solution is written as [2, 3]

$$\Delta T_l(a, t) = \Delta T(a, t) + \frac{fa^2q\lambda_1\alpha_3}{8\pi\lambda_3^2\alpha_1} \ln \frac{4\alpha_3t}{a^2C} + \frac{qfa^2}{16\pi\lambda_3} \left(\frac{-\pi^2}{6} + \ln^2 \frac{4\alpha_3t}{a^2C} \right) - \frac{qf\alpha_3t}{4\pi\lambda_3} - \frac{qf a^2}{8\pi\lambda_3}, \quad (5)$$

where

$$f = \frac{B}{\alpha_3} \quad \text{and} \quad B = \frac{16Kn^2\sigma T_0^3}{(\rho Cp)_3},$$

and K is the mean absorption coefficient and n is the refractive index of the test fluid (both considered independent of temperature) and σ is the Stephan–Boltzmann constant. The difference between the two solutions, though small, is somewhat dependent upon the magnitude of B with a significant influence on thermal diffusivity [2].

In this work, the thickness of the coating deposited on the long and short wires was determined to be different, as SEM micro-photographs of the wires indicate. The influence of this must now be considered. Since the difference in resistance between the long and short wires due to temperature rise can be stated as

$$\Delta R_l - \Delta R_s = R_{l0} \beta \Delta T_l - R_{s0} \beta \Delta T_s \quad (6)$$

where ΔR_l and ΔR_s are the resistance changes, R_{l0} and R_{s0} are the long and short wire resistances at the initial equilibrium temperature; T_0 ; ΔT_l and ΔT_s are the respective temperature differences with β denoting the temperature coefficient of resistance. If there is no diameter difference between the long and short wires, the temperature rise is

$$\Delta T = \frac{\Delta R_l - \Delta R_s}{(R_{l0} - R_{s0}) \beta}. \quad (7)$$

If the radius is a_1 , Eq. (6) can be rewritten as

$$\Delta R_l - \Delta R_s = R_{l0} \beta \Delta T_l - R_{s0} \beta \Delta T_l + R_{s0} \beta \Delta T_l - R_{s0} \beta \Delta T_s, \quad (8)$$

and Eq. (7) as

$$\Delta T' = \frac{\Delta R_l - \Delta R_s}{(R_{l0} - R_{s0}) \beta} + \frac{R_{s0}(\Delta T_l - \Delta T_s)}{(R_{l0} - R_{s0})}, \quad (9)$$

so that

$$\Delta T = \Delta T' - \delta T = \frac{\Delta R_l - \Delta R_s}{(R_{l0} - R_{s0}) \beta}, \quad (10)$$

where

$$\delta T = \frac{R_{s0}(\Delta T_l - \Delta T_s)}{(R_{l0} - R_{s0})}. \quad (11)$$

ΔT is thus the temperature rise of the hot wires assuming both have the same radius, a_1 . Ignoring any differences in the thermophysical properties of the wire, δT , the difference attributable to the differences in radius can be simplified to

$$\delta T = \frac{R_{s0}}{R_{l0} - R_{s0}} \frac{q}{2\pi\lambda} \ln \frac{a_l}{a_s}. \quad (12)$$

The thermal diffusivity of the fluid is often obtained directly [8] from the same measurement as the thermal conductivity through use of Eq. (1) in the form,

$$\alpha = \frac{a^2 C}{4t'} \exp[4\pi\lambda(P, T_r) \Delta T(a, t')/q], \quad (13)$$

where T_r denotes the reference temperature. However, in order to obtain precise values of the thermal diffusivity at the specified thermostat or equilibrium temperature, the temperature coefficient of the thermal conductivity, χ , must first be measured and its influence corrected. Additionally, a “zero” time temperature offset, caused by any small residual bridge imbalance and/or timing effect, must be evaluated and corrected [2–4]. The thermal diffusivity then can be obtained via the slope of the linear fit of ΔT vs. q , i.e.,

$$\alpha = \frac{a^2 C}{4t'} \exp[4\pi\lambda(P, T_0) \Delta T(a, t')/q], \quad (14)$$

where T_0 denotes the thermostat or "zero" time equilibrium temperature and not the reference temperature T_r .

3. EXPERIMENT

A new transient hot-wire instrument was utilized in this work. The measurement circuit and the measurement methods employed are described elsewhere [2-4]. Two wires with nominal diameters of 12.7 μm , each of different length, were used to compensate for end effects. During a previous measurement program on carbon tetrachloride, the cell had become contaminated, leaving the wires and cell coated with a silicon oxide deposit (as determined by SEM electron probe [3]). Despite repeated attempts to clean the cell chemically, the coating was still adherent to the wires. SEM photographs of pieces of the original and coated wires are shown in Figs. 1a to c. The coating can be seen to be somewhat variable and non-uniform, with different thicknesses of coating (Figs. 1b, c and Table I). Wire diameters were measured photometrically and averaged at several axial positions on samples of the wires removed after the present test series.

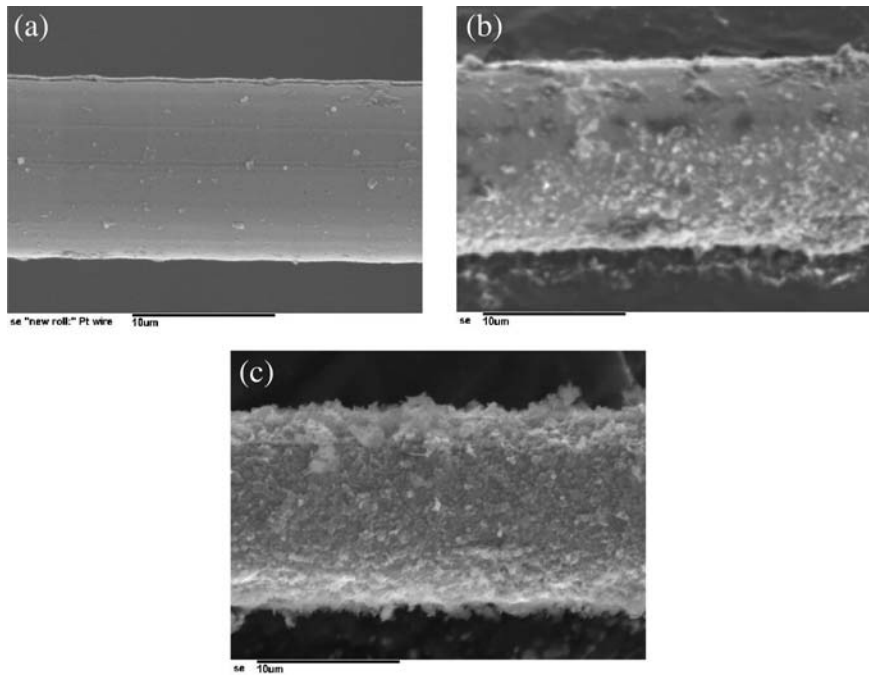


Fig. 1. SEM pictures of hot wires: (a) bare wire; (b) coated short wire; (c) coated long wire.

Table I. Wire and Test Fluid Specifications

(a) Calibration equation: $R = A_0 + A_1 T + A_2 T^2 + B_1 P$; T (°C), P (MPa)		
(b) Wire specification and calibration coefficients; long and short wires		
Purity (%)	99.999	99.999
Length (m)	0.08549 ± 0.00001	0.03395 ± 0.00001
Radius a_2 (μm)	$7.45 \pm 6.8\%$	$7.09 \pm 5.4\%$
Radius a_1 (μm)	$6.53 \pm 1.1\%$	$6.53 \pm 1.1\%$
A_0	62.22233	24.73335
A_1	0.248691	0.0976522
A_2	-6.196378×10^{-5}	-1.688681×10^{-5}
B_1	-1.28134×10^{-3}	-6.27643×10^{-4}
(c) Test Fluid: Toluene; M = 92.134, 99.95% pure		
T_{cr} (593.95 K)	P_{cr} (4.05 MPa)	ρ_{cr} (290 kg · m ⁻³)
(d) Test Fluid: Argon; M = 39.944, 99.999% pure		
T_{cr} (150.86 K)	P_{cr} (5.00 MPa)	ρ_{cr} (536 kg · m ⁻³)

The temperature-resistance characteristics of the wires were determined *in situ* over the temperature and pressure range of the measurements. The wire specifications, as well as the calibration coefficients, are given in Table I, along with the purity and properties of the fluids used.

3.1. Measurements for Argon

To verify the accuracy of the toluene measurements and the validity of the corrections used for the effect of coating and differences in the coating thickness, and thus the wire diameter, the thermal conductivity and thermal diffusivity of argon were measured from 296 to 323 K at pressures to 61 MPa. These measurements are compared with the correlation made from a earlier set of experiments using the same instrument but with uncoated wires [3, 4]. The correlation for thermal conductivity there was given as

$$\lambda(\text{W} \cdot \text{m}^{-1} \cdot \text{K}^{-1}) = \lambda_0 + a_0[1 + a_1 \rho(\text{kg} \cdot \text{m}^{-3}) + a_2(\rho(\text{kg} \cdot \text{m}^{-3}))^2], \quad (15)$$

where

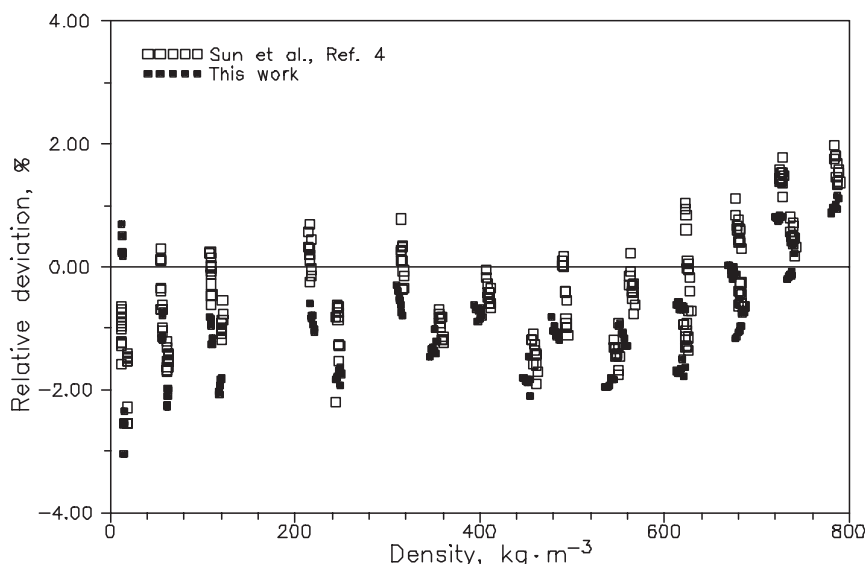
$$\lambda_0 = b_0 + b_1(T(\text{K})) + b_2(T(\text{K}))^2, \quad (16)$$

with the coefficients listed in Table II below.

Table II. Coefficients for Eqs. (15) to (18)

	a_0	a_1	a_2
Argon	1.1212×10^{-4}	2.0516×10^{-5}	2.9472×10^{-8}
Toluene	2.7717×10^{-1}	-8.0377×10^{-4}	7.2520×10^{-7}
	b_0	b_1	b_2
Argon	2.9946×10^{-3}	5.7376×10^{-5}	-2.2458×10^{-8}
Toluene	-1.6158×10^{-3}	6.3469×10^{-6}	1.0104×10^{-7}
	c_0	c_1	c_2
Toluene	26.9377	6.7988×10^{-2}	5.4667×10^{-5}
	d_0	d_1	d_2
Toluene	2189.68	2.16975	-0.0031421

Deviations of the present argon thermal conductivity results from Eq. (15) are shown in Fig. 2, along with the data of Ref. 4 from 296 to 323 K at pressures to 61 MPa. It can be seen that the present data agree well with those measured with the uncoated wires with a maximum deviation of less than 2.5%.

**Fig. 2.** Deviation in the thermal diffusivity of argon from Eq. (15).

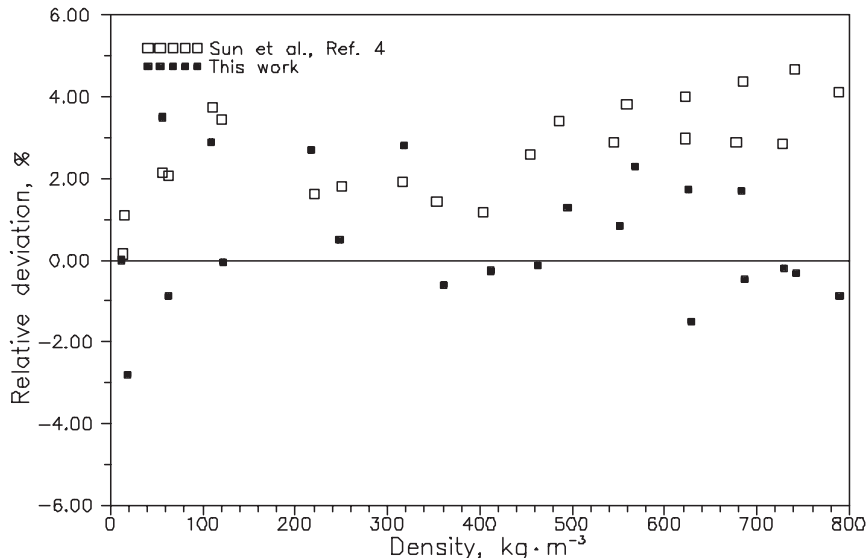


Fig. 3. Deviation in the derived specific heat of argon from that obtained from NIST14 [10].

Via the measured thermal conductivity and thermal diffusivity measurements, and a density determined from Ref. 10, isobaric specific heats were also calculated. The resulting deviation in the present results and the results given by Ref. 4, as compared to values given by Ref. 10, are shown in Fig. 3; the standard deviation of the present data set from the work of Ref. 4 is less than 2%. These measurements and the above comparisons indicate that the corrections due to the influence of the coating and the differences in diameters may be considered valid.

The experimentally determined values of the thermal conductivity of argon from the present measurement program are listed in Table III. The boldfaced type quantities are for the determinations of thermal conductivity, thermal diffusivity, and isobaric specific heat at the equilibrium or bath reference temperature after correcting for the variation in thermal properties and the “zero” time bridge imbalance temperature difference [2–4].

3.2. Measurements for Toluene

The thermal conductivity and thermal diffusivity of toluene were measured along four nominal isotherms, 296, 323, 373, and 423 K at pressures to 35 MPa. These measurements are recorded in Table IV along with their corresponding equilibrium, or T_0 , values. The density values shown

Table III. Thermal Conductivity, Thermal Diffusivity, and Specific Heat of Argon

ID	T (K)	P (kPa)	ρ [10] (kg·m ⁻³)	q (W·m ⁻¹)	λ (W·m ⁻¹ ·K ⁻¹)	$\alpha \times 10^8$ (m ² ·s ⁻¹)	Cp (J·kg ⁻¹ ·K ⁻¹)
	296.97	1136	18.5099		0.01813	188.8	519.0
A20_01C1	297.630	1136	18.4671	0.01451	0.01811		
A20_01D1	297.630	1136	18.4671	0.01452	0.01811		
A20_01A2	298.450	1136	18.4146	0.03263	0.01834		
A20_01B2	298.451	1136	18.4145	0.03264	0.01834		
A20_01C2	299.610	1136	18.3408	0.05801	0.01838		
A20_01D2	299.618	1136	18.3403	0.05801	0.01838		
A20_01A3	301.147	1136	18.2439	0.09074	0.01847		
A20_01B3	301.145	1136	18.2440	0.09072	0.01846		
	296.96	3773	62.4176		0.01928	54.78	563.8
A20_05C1	298.155	3773	62.1371	0.03259	0.01933		
A20_05D1	298.163	3773	62.1353	0.03261	0.01931		
A20_05A2	299.112	3773	61.9151	0.05803	0.01932		
A20_05B2	299.114	3773	61.9146	0.05795	0.01934		
A20_05C2	300.318	3773	61.6377	0.09063	0.01945		
A20_05D2	300.319	3773	61.6375	0.09062	0.01943		
A20_05A3	301.738	3773	61.3146	0.13053	0.01941		
A20_05B3	301.777	3773	61.3058	0.13055	0.01941		
	296.95	7247	121.889		0.02094	27.93	615.1
A20_10C1	297.987	7247	121.372	0.03262	0.02102		
A20_10D1	297.998	7247	121.366	0.03264	0.02095		
A20_10A2	298.785	7247	120.977	0.05791	0.02094		
A20_10B2	298.786	7247	120.976	0.05791	0.02095		
A20_10C2	299.808	7247	120.474	0.09064	0.02096		
A20_10D2	299.808	7247	120.474	0.09060	0.02094		
A20_10A3	300.983	7247	119.904	0.13048	0.02103		
A20_10B3	300.981	7247	119.905	0.13043	0.02101		
	296.55	14454	247.808		0.02472	14.01	712.0
A20_20C1	297.328	14454	246.912	0.03255	0.02484		
A20_20D1	297.329	14454	246.911	0.03260	0.02466		
A20_20E1	297.365	14454	246.87	0.03260	0.02473		
A20_20F1	297.360	14454	246.845	0.03262	0.02488		
A20_20A2	297.950	14454	246.202	0.05790	0.02483		
A20_20B2	297.951	14454	246.2	0.05791	0.02486		
A20_20C2	298.776	14454	245.226	0.09050	0.02489		
A20_20D2	298.809	14454	245.229	0.09050	0.02488		
A20_20A3	299.702	14454	244.227	0.13031	0.02485		
A20_20B3	299.700	14454	244.229	0.13029	0.02450		

Table III. (*Continued*)

ID	T (K)	P (kPa)	ρ [10] (kg·m ⁻³)	q (W·m ⁻¹)	λ (W·m ⁻¹ ·K ⁻¹)	$\alpha \times 10^8$ (m ² ·s ⁻¹)	Cp (J·kg ⁻¹ ·K ⁻¹)
	296.64	21231	361.064		0.02904	10.45	769.7
A20_30C1	297.275	21231	359.958	0.03261	0.02903		
A20_30D1	297.282	21231	359.945	0.03254	0.02905		
A20_30A2	297.780	21231	359.086	0.05791	0.02902		
A20_30B2	297.783	21231	359.081	0.05794	0.02913		
A20_30C2	298.431	21231	357.971	0.09040	0.02911		
A20_30D2	298.436	21231	357.962	0.09042	0.02906		
A20_30A3	299.225	21231	356.621	0.13015	0.02908		
A20_30B3	299.224	21231	356.623	0.13015	0.02906		
A20_30C3	300.103	21231	355.143	0.17715	0.02908		
A20_30D3	300.104	21231	355.141	0.17713	0.0291		
	296.69	27996	462.573		0.03337	8.870	813.3
A20_40C1	297.244	27996	461.383	0.03250	0.03327		
A20_40D1	297.244	27996	461.383	0.03251	0.03343		
A20_40A2	297.683	27996	460.44	0.05783	0.03341		
A20_40B2	297.680	27996	460.446	0.05781	0.03335		
A20_40C2	298.222	27996	459.288	0.09040	0.03343		
A20_40D2	298.221	27996	459.29	0.09035	0.03340		
A20_40A3	298.873	27996	457.905	0.13014	0.03345		
A20_40B3	298.828	27996	458.000	0.13014	0.03329		
A20_40C3	299.616	27996	456.338	0.17715	0.03338		
A20_40D3	299.627	27996	456.315	0.17715	0.03338		
	296.82	34907	551.433		0.03787	8.218	835.6
A20_50C1	297.316	34907	550.244	0.03253	0.03804		
A20_50D1	297.311	34907	550.256	0.03252	0.03772		
A20_50A2	297.691	34907	549.349	0.05794	0.03772		
A20_50B2	297.692	34907	549.346	0.05790	0.03786		
A20_50C2	298.160	34907	548.233	0.09041	0.03777		
A20_50D2	298.160	34907	548.233	0.09040	0.03778		
A20_50A3	298.732	34907	546.879	0.13014	0.03777		
A20_50B3	298.731	34907	546.882	0.13017	0.03772		
A20_50C3	299.372	34907	545.373	0.17716	0.03777		
A20_50D3	299.374	34907	545.368	0.17707	0.03772		
	296.85	41779	626.143		0.04207	7.957	844.4
A20_60C1	297.296	41779	625.036	0.03251	0.04221		
A20_60D1	297.302	41779	625.021	0.03251	0.04194		
A20_60A2	297.626	41779	624.216	0.05780	0.04209		
A20_60B2	297.625	41779	624.219	0.05781	0.04194		
A20_60C2	298.054	41779	623.155	0.09042	0.04200		
A20_60D2	298.052	41779	623.160	0.09040	0.04189		
A20_60A3	298.564	41779	621.896	0.13014	0.04191		
A20_60B3	298.560	41779	621.906	0.13010	0.04189		
A20_60C3	299.167	41779	620.414	0.17712	0.04194		
A20_60D3	299.170	41779	620.406	0.17711	0.04194		

Table III. (*Continued*)

ID	T (K)	P (kPa)	ρ [10] (kg·m ⁻³)	q (W·m ⁻¹)	λ (W·m ⁻¹ ·K ⁻¹)	$\alpha \times 10^8$ (m ² ·s ⁻¹)	Cp (J·kg ⁻¹ ·K ⁻¹)
	296.89	48339	686.675		0.04585	8.130	821.3
A20_70A2	297.593	48339	684.907	0.05781	0.04577		
A20_70B2	297.593	48339	684.907	0.05780	0.04574		
A20_70C2	298.030	48339	683.816	0.09040	0.04575		
A20_70D2	298.029	48339	683.819	0.09036	0.04582		
A20_70A3	298.519	48339	682.600	0.13007	0.04585		
A20_70B3	298.520	48339	682.597	0.13009	0.04570		
A20_70C3	299.091	48339	681.182	0.17697	0.04572		
A20_70D3	299.089	48339	681.187	0.17701	0.04578		
A20_70A4	299.701	48339	679.676	0.23098	0.04566		
A20_70B4	299.658	48339	679.782	0.23101	0.04556		
	296.92	55379	742.331		0.04979	8.229	815.0
A20_80A2	297.577	55379	740.708	0.05780	0.04979		
A20_80B2	297.570	55379	740.725	0.05780	0.04965		
A20_80C2	297.975	55379	739.725	0.09038	0.04970		
A20_80D2	297.974	55379	739.728	0.09040	0.04987		
A20_80A3	298.415	55379	738.641	0.13006	0.04979		
A20_80B3	298.418	55379	738.634	0.13012	0.04970		
A20_80C3	298.935	55379	737.364	0.17703	0.04961		
A20_80D3	298.938	55379	737.357	0.17703	0.04965		
A20_80A4	299.522	55379	735.927	0.23097	0.04962		
A20_80B4	299.548	55379	735.863	0.23096	0.04973		
	296.96	62283	789.544		0.05346	8.436	802.6
A20_90A2	297.564	62283	788.072	0.05783	0.05347		
A20_90B2	297.565	62283	788.070	0.05788	0.05349		
A20_90C2	297.907	62283	787.241	0.09040	0.05333		
A20_90D2	297.917	62283	787.216	0.09035	0.05335		
A20_90A3	298.352	62283	786.164	0.13008	0.05334		
A20_90B3	298.354	62283	786.160	0.13008	0.05346		
A20_90C3	298.871	62283	784.912	0.17700	0.05346		
A20_90D3	298.873	62283	784.907	0.17701	0.05346		
A20_90A4	299.453	62283	783.512	0.23100	0.05348		
A20_90B4	299.449	62283	783.522	0.23097	0.05336		
	322.12	811	12.1357		0.01927	303.3	528.7
A50_01C1	323.244	811	12.0927	0.02461	0.01925		
A50_01D1	323.243	811	12.0927	0.02462	0.01931		
A50_01A2	323.731	811	12.0741	0.03542	0.01934		
A50_01B2	323.711	811	12.0749	0.03540	0.01945		
A50_01C2	324.954	811	12.0278	0.06300	0.01944		
A50_01D2	324.944	811	12.0281	0.06300	0.01945		
A50_01A3	326.507	811	11.9694	0.09852	0.01955		
A50_01B3	326.526	811	11.9687	0.09851	0.01956		
A50_01C3	328.288	811	11.9033	0.14189	0.01961		
A50_01D3	328.282	811	11.9035	0.14185	0.01957		

Table III. (*Continued*)

ID	T (K)	P (kPa)	ρ [10] (kg·m ⁻³)	q (W·m ⁻¹)	λ (W·m ⁻¹ ·K ⁻¹)	$\alpha \times 10^8$ (m ² ·s ⁻¹)	Cp (J·kg ⁻¹ ·K ⁻¹)
	322.16	3679	55.6066		0.02029	63.1	578.3
A50_05A1	323.036	3679	55.4425	0.02460	0.02031		
A50_05B1	323.04	3679	55.4418	0.02460	0.02040		
A50_05C1	323.431	3679	55.3688	0.03541	0.02040		
A50_05D1	323.431	3679	55.3688	0.03540	0.02040		
A50_05A2	324.426	3679	55.184	0.06300	0.02051		
A50_05B2	324.423	3679	55.1846	0.06300	0.02050		
A50_05C2	325.753	3679	54.9397	0.09851	0.02069		
A50_05D2	325.754	3679	54.9375	0.09841	0.02065		
A50_05A3	327.189	3679	54.6779	0.14176	0.02071		
A50_05B3	327.226	3679	54.6712	0.14178	0.02071		
	322.14	7179	109.537		0.02176	32.4	613.1
A50_10A1	322.893	7179	109.239	0.02460	0.02178		
A50_10B1	322.902	7179	109.236	0.02460	0.02187		
A50_10C1	323.231	7179	109.106	0.03541	0.02176		
A50_10D1	323.239	7179	109.103	0.03542	0.02187		
A50_10A2	324.073	7179	108.776	0.06300	0.02192		
A50_10B2	324.078	7179	108.774	0.06292	0.02186		
A50_10C2	325.153	7179	108.355	0.09841	0.02199		
A50_10D2	325.153	7179	108.355	0.09840	0.02196		
A50_10A3	326.419	7179	107.867	0.14174	0.02205		
A50_10B3	326.441	7179	107.859	0.14173	0.02205		
	322.13	14151	217.318		0.02510	16.91	683.0
A50_20A1	322.741	14151	216.79	0.02461	0.02523		
A50_20B1	322.741	14151	216.79	0.02463	0.02508		
A50_20C1	323.012	14151	216.557	0.03540	0.02506		
A50_20D1	323.022	14151	216.549	0.03542	0.02515		
A50_20A2	323.683	14151	215.984	0.06290	0.02518		
A50_20B2	323.684	14151	215.983	0.06290	0.02518		
A50_20C2	324.526	14151	215.268	0.09841	0.02522		
A50_20D2	324.598	14151	215.207	0.09842	0.02532		
A50_20A3	325.554	14151	214.402	0.14165	0.02524		
A50_20B3	325.559	14151	214.398	0.14168	0.02530		
	322.11	20909	317.732		0.02871	12.23	738.8
A50_30A1	322.629	20909	317.06	0.02458	0.02873		
A50_30B1	322.637	20909	317.05	0.02459	0.02865		
A50_30C1	322.870	20909	316.747	0.03541	0.02864		
A50_30D1	322.868	20909	316.75	0.03538	0.02884		
A50_30A2	323.436	20909	316.014	0.06300	0.02884		
A50_30B2	323.434	20909	316.017	0.06301	0.02877		
A50_30C2	324.148	20909	315.098	0.09840	0.02881		
A50_30D2	324.169	20909	315.071	0.09839	0.02896		
A50_30A3	324.961	20909	314.059	0.14167	0.02881		
A50_30B3	324.959	20909	314.062	0.14169	0.02876		

Table III. (*Continued*)

ID	<i>T</i> (K)	<i>P</i> (kPa)	ρ [10] (kg·m ⁻³)	<i>q</i> (W·m ⁻¹)	λ (W·m ⁻¹ ·K ⁻¹)	$\alpha \times 10^8$ (m ² ·s ⁻¹)	Cp (J·kg ⁻¹ ·K ⁻¹)
	322.11	27855	412.275		0.03251	10.11	714.1
A50_40C1	322.752	27855	411.209	0.03550	0.03259		
A50_40D1	322.753	27855	411.207	0.03551	0.03251		
A50_40A2	323.249	27855	410.384	0.06300	0.0325		
A50_40B2	323.246	27855	410.389	0.06300	0.03252		
A50_40C2	323.837	27855	409.414	0.09841	0.03253		
A50_40D2	323.864	27855	409.369	0.09840	0.03253		
A50_40A3	324.560	27855	408.227	0.14171	0.03256		
A50_40B3	324.580	27855	408.194	0.14172	0.03249		
A50_40C3	325.434	27855	406.803	0.19284	0.03257		
A50_40D3	325.441	27855	406.792	0.19282	0.03261		
	322.09	34713	494.94		0.03622	9.292	787.6
A50_50C1	322.635	34713	493.889	0.03540	0.03640		
A50_50D1	322.638	34713	493.883	0.03540	0.03624		
A50_50A2	323.071	34713	493.059	0.06300	0.03624		
A50_50B2	323.067	34713	493.067	0.06299	0.03627		
A50_50C2	323.655	34713	491.953	0.09841	0.03640		
A50_50D2	323.658	34713	491.947	0.09840	0.03640		
A50_50A3	324.332	34713	490.677	0.14162	0.03652		
A50_50B3	324.374	34713	490.598	0.14163	0.03658		
A50_50C3	325.100	34713	489.238	0.19273	0.03649		
A50_50D3	325.093	34713	489.251	0.19272	0.03651		
	322.1	41648	567.591		0.04015	8.794	804.4
A50_60C1	322.598	41648	566.564	0.03540	0.04005		
A50_60D1	322.605	41648	566.549	0.03540	0.04025		
A50_60A2	322.992	41648	565.758	0.06298	0.04017		
A50_60B2	323.012	41648	565.717	0.06300	0.04013		
A50_60C2	323.491	41648	564.741	0.09842	0.04018		
A50_50D2	323.486	41648	564.752	0.09840	0.04014		
A50_60A3	324.156	41648	563.393	0.14167	0.04035		
A50_60B3	324.137	41648	563.431	0.14165	0.04023		
A50_60C3	324.737	41648	562.220	0.19273	0.04010		
A50_60D3	324.728	41648	562.238	0.19273	0.04016		
	322.11	48371	628.699		0.04349	8.914	776.3
A50_70A2	322.925	48371	626.983	0.06290	0.04367		
A50_70B2	322.934	48371	626.964	0.06290	0.04357		
A50_70C2	323.396	48371	625.992	0.09830	0.04373		
A50_70D2	323.416	48371	625.950	0.09840	0.04368		
A50_70A3	323.939	48371	624.854	0.14157	0.04365		
A50_70B3	323.944	48371	624.843	0.14162	0.04370		
A50_70A4	324.679	48371	623.309	0.19273	0.04397		
A50_70B4	324.679	48371	623.309	0.19271	0.04387		
A50_70C4	325.434	48371	621.740	0.25147	0.04396		
A50_70D4	325.437	48371	621.734	0.25148	0.04400		

Table III. (Continued)

ID	T (K)	P (kPa)	$\rho [10]$ (kg·m ⁻³)	q (W·m ⁻¹)	λ (W·m ⁻¹ ·K ⁻¹)	$\alpha \times 10^8$ (m ² ·s ⁻¹)	Cp (J·kg ⁻¹ ·K ⁻¹)
	322.1	55241	683.241		0.04717	8.675	795.8
A50_80A2	322.845	55241	681.642	0.06301	0.04725		
A50_80B2	322.845	55241	681.642	0.06298	0.04717		
A50_80C2	323.254	55241	680.773	0.09840	0.04712		
A50_80D2	323.288	55241	680.700	0.09838	0.04722		
A50_80A3	323.803	55241	679.608	0.14161	0.04725		
A50_80B3	323.810	55241	679.593	0.1416	0.04709		
A50_80C3	324.394	55241	678.359	0.19266	0.04712		
A50_80D3	324.401	55241	678.344	0.19267	0.04715		
A50_80A4	325.079	55241	676.917	0.25139	0.04717		
A50_80B4	325.081	55241	676.913	0.25136	0.04730		
	322.07	61752	728.823		0.0506	8.893	780.7
A50_90C1	322.443	61752	728.019	0.03540	0.05072		
A50_90D1	322.449	61752	728.007	0.03540	0.05059		
A50_90A2	322.754	61752	727.358	0.06292	0.05037		
A50_90B2	322.763	61752	727.339	0.06290	0.05048		
A50_90C2	323.162	61752	726.492	0.09833	0.05053		
A50_90D2	323.175	61752	726.465	0.09828	0.05047		
A50_90A3	323.693	61752	725.368	0.14148	0.05040		
A50_90B3	323.698	61752	725.358	0.14142	0.05043		
A50_90C3	324.281	61752	724.127	0.19244	0.05037		
A50_90D3	324.282	61752	724.125	0.19252	0.05045		

were calculated from Ref. 11. The over 253 individual experimental data points for thermal conductivity were used to establish 24 determinations of thermal diffusivity and specific heat. The derived values of thermal conductivity, thermal diffusivity, and specific heat, at the established thermostat equilibrium temperatures are indicated in boldfaced type. In addition, values of B , which account for the influence of fluid thermal radiation are also listed.

Deviations in the temperature rise of the hot wire from the linear fit of ΔT vs. $\ln(t)$ before and after correcting for the influence of fluid thermal radiation are shown in Fig. 4 for a measurement at 323 K and 20 MPa (ID# T50_30A7). Here, it can be seen that before correction, a systematic convex curvature in the data exists out to 3 s that cannot be explained by free convection since Ra is only 1.92×10^4 and much less than “critical” [12]. Although the maximum deviation over this time period is smaller than 0.1%, its curvature is very distinct and can only be eliminated through use of a value of $B = 0.0088 \text{ s}^{-1}$; this procedure decreases the maximum

Table IV. Thermal Conductivity, Thermal Diffusivity, and Specific Heat of Toluene

Id No.	T (K)	P (kPa)	ρ [10] (kg·m ⁻³)	q (W·m ⁻¹)	λ (W·m ⁻¹ ·K ⁻¹)	$\alpha \times 10^8$ (m ² ·s ⁻¹)	Cp (J·kg ⁻¹ ·K ⁻¹)	B (s ⁻¹)
	297.46	3357	869.404		0.1332	9.003	1702	
T20_05A3	297.991	3357	868.887	0.12403	0.1330			0.005
T20_05B3	297.992	3357	868.887	0.12403	0.1330			0.005
T20_05A4	298.412	3357	868.492	0.21999	0.1327			0.005
T20_05B4	298.414	3357	868.488	0.22008	0.1328			0.005
T20_05A5	298.942	3357	867.982	0.34328	0.1326			0.005
T20_05B5	298.951	3357	867.979	0.34324	0.1326			0.005
T20_05A6	299.585	3357	867.360	0.49339	0.1323			0.005
T20_05B6	299.579	3357	867.359	0.49336	0.1324			0.005
T20_05A7	300.343	3357	866.633	0.66957	0.1322			0.005
T20_06B7	300.345	3357	866.634	0.66955	0.1322			0.005
	297.46	6763	872.023		0.1346	9.229	1672	
T20_10A5	298.935	6763	870.635	0.34319	0.1340			0.0045
T20_10B5	298.933	6763	870.637	0.34321	0.1340			0.0045
T20_10A6	299.581	6763	870.031	0.49328	0.1337			0.0045
T20_10B6	299.583	6763	870.031	0.49322	0.1337			0.0045
T20_10A8	301.192	6763	868.504	0.87237	0.1330			0.0045
T20_10B8	301.234	6763	868.452	0.87238	0.1330			0.0045
	297.50	13637	877.075		0.1369	9.369	1666	
T20_20A3	298.034	13637	876.590	0.12401	0.1369			0.0045
T20_20B3	298.032	13637	876.590	0.12403	0.1369			0.0045
T20_20A4	298.431	13637	876.218	0.22003	0.1364			0.0045
T20_20B4	298.462	13637	876.196	0.22003	0.1363			0.0045
T20_20A5	298.953	13637	875.743	0.34329	0.1364			0.0045
T20_20B5	298.954	13637	875.743	0.34329	0.1364			0.0045
T20_20A6	299.585	13637	875.167	0.49341	0.1362			0.0045
T20_20B6	299.581	13637	875.167	0.49341	0.1362			0.0045
T20_20A7	300.424	13637	874.391	0.66982	0.1358			0.0045
T20_20B7	300.369	13637	874.450	0.66976	0.1359			0.0045
T20_20A8	301.175	13637	873.706	0.87253	0.1356			0.0045
T20_20B8	301.172	13637	873.707	0.87239	0.1356			0.0045
	297.57	20565	881.884		0.1395	9.563	1654	
T20_30A3	298.092	20565	881.419	0.12397	0.1392			0.004
T20_30A5	299.011	20565	880.606	0.34375	0.1386			0.004
T20_30A6	299.632	20565	880.048	0.49412	0.1384			0.004
	297.56	27349	886.445		0.1412	9.625	1655	
T20_40A3	298.081	27349	885.990	0.12412	0.1409			0.004
T20_40B3	298.083	27349	885.990	0.12412	0.1409			0.004
T20_40A4	298.484	27349	885.652	0.22031	0.1410			0.004

Table IV. (*Continued*)

Id No.	T (K)	P (kPa)	ρ [10] (kg·m ⁻³)	q (W·m ⁻¹)	λ (W·m ⁻¹ ·K ⁻¹)	$\alpha \times 10^8$ (m ² ·s ⁻¹)	Cp (J·kg ⁻¹ ·K ⁻¹)	B (s ⁻¹)
T20_40B4	298.479	27349	885.653	0.22024	0.1410			0.004
T20_40A5	299.583	27349	884.688	0.49405	0.1407			0.004
T20_40B5	299.571	27349	884.691	0.49406	0.1406			0.004
T20_40A6	300.293	27349	884.065	0.67070	0.1404			0.004
T20_40B6	300.303	27349	884.065	0.67074	0.1404			0.004
T20_40A7	301.131	27349	883.347	0.87359	0.1401			0.004
T20_40B7	301.114	27349	883.353	0.87367	0.1402			0.004
	297.50	34320	890.965	0.22035	0.1434	9.684	1662	
T20_50A4	298.421	34320	890.188	0.22035	0.1433			0.0038
T20_50B4	298.424	34320	890.191	0.22042	0.1429			0.0038
T20_50A5	298.902	34320	889.757	0.34380	0.1430			0.0038
T20_50B5	298.911	34320	889.774	0.34380	0.1430			0.0038
T20_50A6	299.532	34320	889.263	0.49421	0.1427			0.0038
T20_50B6	299.534	34320	889.266	0.49414	0.1428			0.0038
T20_50A7	300.271	34320	888.609	0.67067	0.1425			0.0038
T20_50B7	300.273	34320	888.609	0.67067	0.1425			0.0038
T20_50A8	301.140	34320	887.875	0.87354	0.1422			0.0038
T20_50B8	301.134	34320	887.879	0.87330	0.1422			0.0038
	327.67	3364	840.234		0.1248	8.364	1776	
T50_05A3	328.231	3364	839.684	0.12662	0.1248			0.008
T50_05B3	328.223	3364	839.694	0.12663	0.1244			0.008
T50_05A4	328.674	3364	839.259	0.22472	0.1246			0.008
T50_05B4	328.662	3364	839.267	0.22469	0.1245			0.008
T50_05A5	329.234	3364	838.711	0.35062	0.1243			0.008
T50_05B5	329.275	3364	838.685	0.35063	0.1243			0.008
T50_05A6	329.953	3364	838.020	0.50398	0.1241			0.008
T50_05B6	329.961	3364	838.009	0.50407	0.1241			0.008
T50_05A7	330.783	3364	837.208	0.68441	0.1239			0.0085
T50_05B7	330.832	3364	837.162	0.68430	0.1239			0.0085
T50_05A8	331.772	3364	836.238	0.89171	0.1236			0.009
T50_05B8	331.800	3364	836.220	0.89161	0.1237			0.009
	327.68	6754	843.332		0.1260	8.516	1754	
T50_10A3	328.281	6754	842.764	0.12660	0.1259			0.0085
T50_10B3	328.220	6754	842.814	0.12651	0.1259			0.008
T50_10A4	328.689	6754	842.378	0.22455	0.1257			0.008
T50_10B4	328.750	6754	842.363	0.22459	0.1258			0.008
T50_10A5	329.263	6754	841.829	0.35042	0.1257			0.008
T50_10B5	329.261	6754	841.837	0.35042	0.1257			0.0085
T50_10A6	329.940	6754	841.173	0.50374	0.1255			0.0085
T50_10B6	329.943	6754	841.175	0.50370	0.1255			0.0085
T50_10A7	330.764	6754	840.394	0.68411	0.1253			0.0085

Table IV. (*Continued*)

Id No.	T (K)	P (kPa)	ρ [10] (kg·m ⁻³)	q (W·m ⁻¹)	λ (W·m ⁻¹ ·K ⁻¹)	$\alpha \times 10^8$ (m ² ·s ⁻¹)	Cp (J·kg ⁻¹ ·K ⁻¹)	B (s ⁻¹)
T50_10B7	330.769	6754	840.393	0.68421	0.1253			0.0087
T50_10A8	331.758	6754	839.492	0.89149	0.1251			0.0092
T50_10B8	331.765	6754	839.494	0.89155	0.1250			0.009
	327.52	13813	849.64		0.1288	8.805	1722	
T50_20A3	328.141	13813	849.076	0.12667	0.1285			0.008
T50_20B3	328.144	13813	849.068	0.12669	0.1288			0.008
T50_20A4	328.560	13813	848.684	0.22479	0.1285			0.0075
T50_20B4	328.529	13813	848.723	0.22474	0.1285			0.0075
T50_20A5	329.094	13813	848.198	0.35080	0.1284			0.0086
T50_20B5	329.073	13813	848.213	0.35063	0.1284			0.0085
T50_20A6	329.734	13813	847.622	0.50398	0.1282			0.0083
T50_20B6	329.728	13813	847.621	0.50384	0.1282			0.0086
T50_20A7	330.513	13813	846.888	0.68433	0.1280			0.0086
T50_20B7	330.532	13813	846.875	0.68458	0.1280			0.0085
T50_20A8	331.451	13813	846.028	0.89151	0.1278			0.0088
T50_20B8	331.460	13813	846.020	0.89113	0.1278			0.0088
	327.51	20548	855.173		0.1312	8.882	1727	
T50_30A3	328.082	20548	854.67	0.12666	0.1309			0.007
T50_30B3	328.091	20548	854.665	0.12665	0.1314			0.008
T50_30A4	328.522	20548	854.288	0.22480	0.1310			0.008
T50_30B4	328.534	20548	854.295	0.22482	0.1310			0.0082
T50_30A5	329.048	20548	853.811	0.35081	0.1309			0.0078
T50_30B5	329.041	20548	853.818	0.35075	0.1309			0.0082
T50_30A6	329.700	20548	853.225	0.50420	0.1307			0.0082
T50_30B6	329.700	20548	853.23	0.50413	0.1307			0.0075
T50_30A7	330.481	20548	852.231	0.68443	0.1306			0.0082
T50_30B7	330.493	20548	852.526	0.68447	0.1305			0.0082
T50_30A8	331.381	20548	851.73	0.89153	0.1303			0.0087
T50_30B8	331.392	20548	851.715	0.89157	0.1303			0.0087
	327.58	27320	860.367		0.1335	8.92	1740	
T50_40A3	328.142	27320	859.883	0.12652	0.1334			0.0084
T50_40B3	328.140	27320	859.883	0.12652	0.1334			0.008
T50_40A4	328.532	27320	859.550	0.22460	0.1334			0.008
T50_40B4	328.534	27320	859.550	0.22460	0.1334			0.008
T50_40A5	329.081	27320	859.081	0.35041	0.1333			0.0075
T50_40B5	329.073	27320	859.075	0.35043	0.1332			0.0075
T50_40A6	329.732	27320	858.508	0.50370	0.1330			0.0082
T50_40B6	329.731	27320	858.507	0.50373	0.1330			0.0082
T50_40A7	330.554	27320	857.796	0.68392	0.1330			0.008
T50_40B7	330.559	27320	857.801	0.68379	0.1329			0.008
T50_40A8	331.891	27320	856.649	1.00431	0.1326			0.008
T50_40B8	331.886	27320	856.651	1.00411	0.1326			0.009

Table IV. (*Continued*)

Id No.	T (K)	P (kPa)	ρ [10] (kg·m ⁻³)	q (W·m ⁻¹)	λ (W·m ⁻¹ ·K ⁻¹)	$\alpha \times 10^8$ (m ² ·s ⁻¹)	Cp (J·kg ⁻¹ ·K ⁻¹)	B (s ⁻¹)
	327.63	34404	865.54		0.1362	8.914	1737	
T50_50A3	328.190	34404	865.105	0.12652	0.1361			0.008
T50_50B3	328.193	34404	865.096	0.12647	0.136			0.008
T50_50A4	329.161	34404	864.303	0.35025	0.1358			0.008
T50_50B4	329.162	34404	864.302	0.35023	0.1358			0.008
T50_50A5	329.830	34404	863.762	0.50351	0.1357			0.008
T50_50B5	329.833	34404	863.762	0.50351	0.1357			0.0082
T50_50A6	330.654	34404	863.120	0.68352	0.1355			0.0082
T50_50B6	330.661	34404	863.129	0.68356	0.1355			0.008
T50_50A7	331.494	34404	862.396	0.89054	0.1353			0.0085
T50_50B7	331.497	34404	862.393	0.89037	0.1353			0.0085
T50_50A8	333.600	34404	860.670	1.38239	0.1348			0.0088
T50_50B8	333.611	34404	860.670	1.38247	0.1348			0.0088
	378.44	3492	790.087		0.1104	7.397	1889	
T10_05A3	378.782	3492	790.044	0.14680	0.1105			0.026
T10_05B3	378.783	3492	789.748	0.14677	0.1104			0.030
T10_05A4	380.037	3492	788.471	0.26044	0.1101			0.032
T10_05B4	380.033	3492	788.478	0.26032	0.1101			0.030
T10_05A5	380.751	3492	787.735	0.40610	0.1100			0.030
T10_05B5	380.770	3492	787.723	0.40607	0.1098			0.030
T10_05A6	381.684	3492	786.788	0.58326	0.1098			0.026
T10_05B6	381.700	3492	786.787	0.58349	0.1098			0.026
T10_05A7	382.793	3492	785.659	0.79178	0.1097			0.030
T10_05B7	382.841	3492	785.614	0.79201	0.1097			0.030
	378.76	7293	794.545		0.1122	7.454	1894	
T10_10A3	379.571	7293	793.753	0.14682	0.1122			0.032
T10_10B3	379.542	7293	793.774	0.14676	0.1119			0.045
T10_10A4	380.160	7293	793.182	0.26043	0.1121			0.032
T10_10B4	380.141	7293	793.183	0.26041	0.1120			0.034
T10_10A5	380.792	7293	792.555	0.40617	0.1119			0.034
T10_10B5	380.751	7293	792.594	0.40612	0.1116			0.034
T10_10A6	381.590	7293	791.755	0.58339	0.1116			0.034
T10_10B6	381.593	7293	791.759	0.58350	0.1115			0.036
T10_10A7	382.559	7293	790.799	0.79190	0.1115			0.036
T10_10B7	382.671	7293	790.707	0.79180	0.1115			0.032
T10_10A8	384.056	7293	789.319	1.03145	0.1116			0.032
T10_10B8	384.057	7293	789.325	1.03155	0.1116			0.034
	378.84	13694	801.976		0.1152	7.518	1910	
T10_20A3	379.571	13694	801.289	0.14668	0.1149			0.026
T10_20B3	379.590	13694	801.274	0.14670	0.1151			0.024

Table IV. (*Continued*)

Id No.	T (K)	P (kPa)	ρ [10] (kg·m ⁻³)	q (W·m ⁻¹)	λ (W·m ⁻¹ ·K ⁻¹)	$\alpha \times 10^8$ (m ² ·s ⁻¹)	Cp (J·kg ⁻¹ ·K ⁻¹)	B (s ⁻¹)
T10_20A4	380.193	13694	800.709	0.26040	0.1152			0.025
T10_20B4	380.175	13694	800.735	0.26042	0.1152			0.025
T10_20A5	380.822	13694	800.123	0.40613	0.1147			0.025
T10_20B5	380.821	13694	800.124	0.40579	0.1146			0.025
T10_20A6	381.760	13694	799.232	0.58302	0.1146			0.025
T10_20B6	381.855	13694	799.2	0.58318	0.1147			0.032
T10_20A7	381.780	13694	799.226	0.79124	0.1145			0.028
T10_20B7	381.821	13694	799.162	0.79128	0.1145			0.028
T10_20A8	383.889	13694	797.242	1.03064	0.1144			0.028
T10_20B8	383.890	13694	797.243	1.03047	0.1143			0.028
	378.81	20553	809.414		0.1181	7.702	1894	
T10_30A3	379.621	20553	808.685	0.14660	0.1181			0.023
T10_30B3	379.614	20553	808.692	0.14661	0.1181			0.023
T10_30A4	380.072	20553	808.28	0.26052	0.1178			0.023
T10_30B4	380.100	20553	808.259	0.26037	0.1180			0.024
T10_30A5	380.780	20553	807.644	0.40598	0.1177			0.025
T10_30B5	380.781	20553	807.656	0.40588	0.1176			0.025
T10_30A6	381.583	20553	806.939	0.58318	0.1176			0.023
T10_30B6	381.562	20553	806.95	0.58313	0.1175			0.025
T10_30A7	382.631	20553	805.985	0.79086	0.1174			0.025
T10_30B7	382.640	20553	805.982	0.79106	0.1174			0.025
T10_30A8	383.594	20553	805.124	1.03008	0.1173			0.030
T10_30B8	383.594	20553	805.123	1.03013	0.1173			0.030
	378.79	27407	816.288		0.1207	7.805	1894	
T10_40A3	379.511	27407	815.667	0.14659	0.1208			0.015
T10_40B3	379.524	27407	815.658	0.14661	0.1207			0.015
T10_40A4	380.052	27407	815.203	0.26024	0.1205			0.020
T10_40B4	380.045	27407	815.217	0.26028	0.1205			0.020
T10_40A5	380.732	27407	814.625	0.40598	0.1203			0.025
T10_40B5	380.731	27407	814.641	0.40594	0.1203			0.025
T10_40A6	381.522	27407	813.932	0.58314	0.1202			0.025
T10_40B6	381.490	27407	813.961	0.58301	0.1202			0.027
T10_40A7	382.561	27407	813.036	0.79112	0.1202			0.025
T10_40B7	382.554	27407	813.046	0.19107	0.1202			0.025
T10_40A8	383.782	27407	811.988	1.03010	0.1201			0.028
T10_40B8	383.788	27407	811.98	1.03008	0.1201			0.028
	378.86	34368	822.727		0.1232	7.941	1886	
T10_50A3	379.461	34368	822.228	0.14653	0.1234			0.020
T10_50B3	379.493	34368	822.203	0.14662	0.1229			0.020
T10_50A4	380.000	34368	821.780	0.26024	0.1232			0.015

Table IV. (*Continued*)

Id No.	T (K)	P (kPa)	ρ [10] (kg·m ⁻³)	q (W·m ⁻¹)	λ (W·m ⁻¹ ·K ⁻¹)	$\alpha \times 10^8$ (m ² ·s ⁻¹)	Cp (J·kg ⁻¹ ·K ⁻¹)	B (s ⁻¹)
T10_50B4	380.000	34368	821.780	0.26024	0.1232			0.020
T10_50A5	380.763	34368	821.148	0.40615	0.1231			0.017
T10_50B5	380.809	34368	821.106	0.40611	0.1231			0.020
T10_50A6	381.517	34368	820.517	0.58362	0.1231			0.020
T10_50B6	381.520	34368	820.517	0.58361	0.1231			0.022
T10_50A7	382.591	34368	819.628	0.79191	0.1232			0.022
T10_50B7	382.599	34368	819.628	0.79191	0.1232			0.022
T10_50A8	383.322	34368	819.013	1.03129	0.1230			0.025
T10_50B8	383.328	34368	819.012	1.03130	0.1230			0.025
	423.91	3415	742.166		0.1	6.541	2060	
T15_05A3	424.971	3415	741.008	0.16440	0.1002			0.040
T15_05B3	424.955	3415	741.009	0.16437	0.1002			0.042
T15_05A4	425.673	3415	740.238	0.29164	0.09997			0.054
T15_05B4	425.552	3415	740.349	0.29162	0.09942			0.051
T15_05A5	426.353	3415	739.471	0.45459	0.09900			0.054
T15_05B5	426.345	3415	739.479	0.45453	0.09967			0.056
T15_05A6	427.341	3415	738.379	0.65285	0.09973			0.054
T15_05B6	427.340	3415	738.378	0.65289	0.09971			0.050
T15_05A7	428.554	3415	737.051	0.88579	0.09948			0.052
T15_05B7	428.611	3415	736.972	0.88590	0.09949			0.054
	423.74	6825	748.31		0.1020	6.713	2030	
T15_10A3	424.710	6825	747.29	0.16427	0.1021			0.040
T15_10B3	424.721	6825	747.287	0.16429	0.1021			0.040
T15_10A4	425.390	6825	746.573	0.29142	0.1016			0.050
T15_10B4	425.410	6825	746.561	0.29141	0.1019			0.050
T15_10A5	426.191	6825	745.73	0.45437	0.1018			0.050
T15_10B5	426.140	6825	745.783	0.45442	0.1017			0.050
T15_10A6	427.122	6825	744.749	0.65246	0.1018			0.054
T15_10B6	427.132	6825	744.748	0.65258	0.1018			0.052
T15_10A7	428.419	6825	743.375	0.88520	0.1017			0.055
T15_10B7	428.444	6825	743.364	0.88519	0.1018			0.048
	423.92	13833	759.182		0.1053	6.879	2016	μ
T15_20A3	424.793	13833	758.335	0.16444	0.1054			0.031
T15_20B3	424.790	13833	758.340	0.16441	0.1053			0.038
T15_20A4	425.474	13833	757.674	0.29162	0.1054			0.033
T15_20B4	425.498	13833	757.643	0.29168	0.1055			0.041
T15_20A5	426.322	13833	756.843	0.45478	0.1055			0.040
T15_20B5	426.312	13833	756.852	0.45486	0.1056			0.040
T15_20A6	427.364	13833	755.827	0.65344	0.1055			0.045
T15_20B6	427.321	13833	755.868	0.65363	0.1057			0.040

Table IV. (*Continued*)

Id No.	<i>T</i> (K)	<i>P</i> (kPa)	ρ [10] (kg·m ⁻³)	<i>q</i> (W·m ⁻¹)	λ (W·m ⁻¹ ·K ⁻¹)	$\alpha \times 10^8$ (m ² ·s ⁻¹)	Cp (J·kg ⁻¹ ·K ⁻¹)	B (s ⁻¹)
T15_20A7	428.511	13833	754.704	0.88653	0.1058			0.045
T15_20B7	428.580	13833	754.640	0.88653	0.1058			0.042
	423.91	20592	768.654		0.1086	7.041	2007	
T15_30A3	424.814	20592	767.829	0.16449	0.1086			0.030
T15_30B3	424.811	20592	767.834	0.16445	0.1086			0.035
T15_30A4	425.433	20592	767.262	0.29180	0.1087			0.034
T15_30B4	425.414	20592	767.277	0.29176	0.1086			0.035
T15_30A5	426.241	20592	766.516	0.45484	0.1087			0.037
T15_30B5	426.249	20592	766.514	0.45488	0.1085			0.035
T15_30A6	427.308	20592	765.537	0.65341	0.1086			0.035
T15_30B6	427.311	20592	765.538	0.65324	0.1086			0.040
T15_30A7	428.413	20592	764.527	0.88609	0.1086			0.045
T15_30B7	428.444	20592	764.500	0.88583	0.1085			0.045
	423.95	27597	777.474		0.1118	7.081	2031	
T15_40A3	424.832	27597	776.709	0.16442	0.1119			0.025
T15_40B3	424.838	27597	776.706	0.16438	0.1117			0.025
T15_40A4	425.445	27597	776.176	0.29159	0.1117			0.034
T15_40B4	425.423	27597	776.196	0.29154	0.1119			0.028
T15_40A5	426.259	27597	775.473	0.45462	0.1118			0.031
T15_40B5	426.254	27597	775.476	0.45439	0.1118			0.036
T15_40A6	427.211	27597	774.647	0.65277	0.1116			0.037
T15_40B6	427.230	27597	774.624	0.65289	0.1118			0.036
T15_40A7	428.444	27597	773.576	0.88561	0.1119			0.040
T15_40B7	428.432	27597	773.581	0.88554	0.1119			0.040
	423.92	34408	785.372		0.1143	7.181	2026	
T15_50A3	424.781	34408	784.658	0.16431	0.1143			0.025
T15_50B3	424.782	34408	784.660	0.16435	0.1142			0.025
T15_50A4	425.383	34408	784.160	0.29153	0.1146			0.027
T15_50B4	425.390	34408	783.783	0.29154	0.1148			0.031
T15_50A5	426.111	34408	783.553	0.45451	0.1147			0.029
T15_50B5	426.100	34408	783.563	0.45451	0.1148			0.031
T15_50A6	427.091	34408	782.746	0.65281	0.1148			0.035
T15_50B6	427.144	34408	782.704	0.65279	0.1149			0.035
T15_50A7	428.181	34408	781.837	0.88562	0.1149			0.035
T15_50B7	428.300	34408	781.736	0.88558	0.1150			0.037

deviation in the linear fit to less than $\pm 0.01\%$. The change in the value of thermal conductivity due to this correction is only 0.8%; however, the thermal diffusivity changes by -5.6% , emphasizing the importance of this correction for this property.

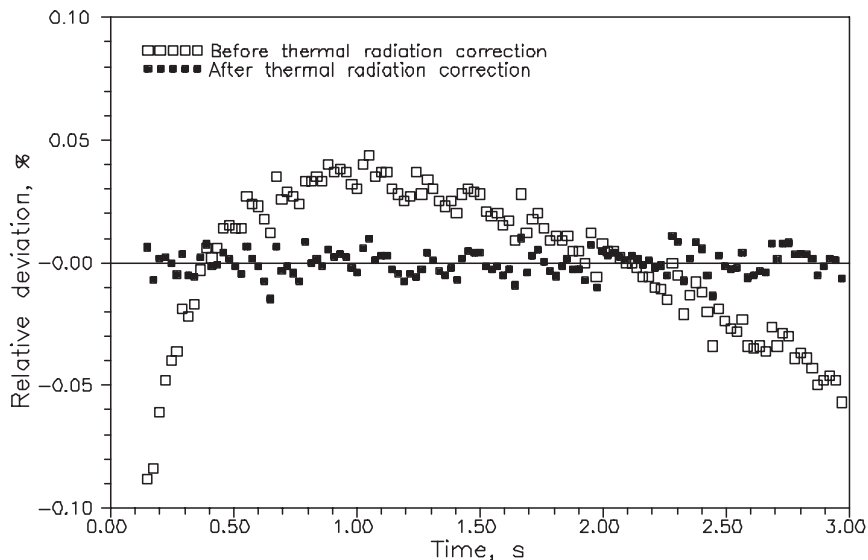


Fig. 4. Deviation in the temperature rise from the best linear fit of $\Delta T \sim \ln(t)$ for a measurement of toluene at 323 K and 20 MPa (Run ID T50_50A7) before and after correcting for the influence of fluid thermal radiation; $B = 0.0088 \text{ s}^{-1}$.

3.2.1. Thermal Conductivity

The experimental thermal conductivity values were correlated with equations of the form of Eqs. (15) and (16) where λ_0 values were obtained via Ref. 11 by setting pressure to zero and correlated vs. temperature; the coefficients used are given in Table II.

The present thermal conductivity data and those from other sources are shown in Fig. 5. The deviations of all these data from Eq. (15) are shown in Fig. 6. The maximum deviation of the present data from the correlation is about 1.5% with a standard deviation of only $\pm 0.7\%$; the majority of the other data deviates, at most, by 3%.

Perkins et al. [8] made thermal conductivity and diffusivity measurements from 302 to 555 K at pressures from 0.09 to 20 MPa. Ramires et al. [13] and Nieto de Castro et al. [9] measured only the thermal conductivity along the saturation line from 300 to 381 K and 300 to 550 K, respectively. Nieto de Castro et al. [7] measured the thermal conductivity from 308 to 363 K with pressures to 0.53 GPa. Mani and Venart [14] measured only the thermal conductivity from 300 to 590 K at pressures to 14 MPa. All of this work utilized transient hot wire instruments where the influence of fluid radiation was taken into account, except for that of Mani and Venart [14]. Shulga et al. [15] made measurements of both thermal

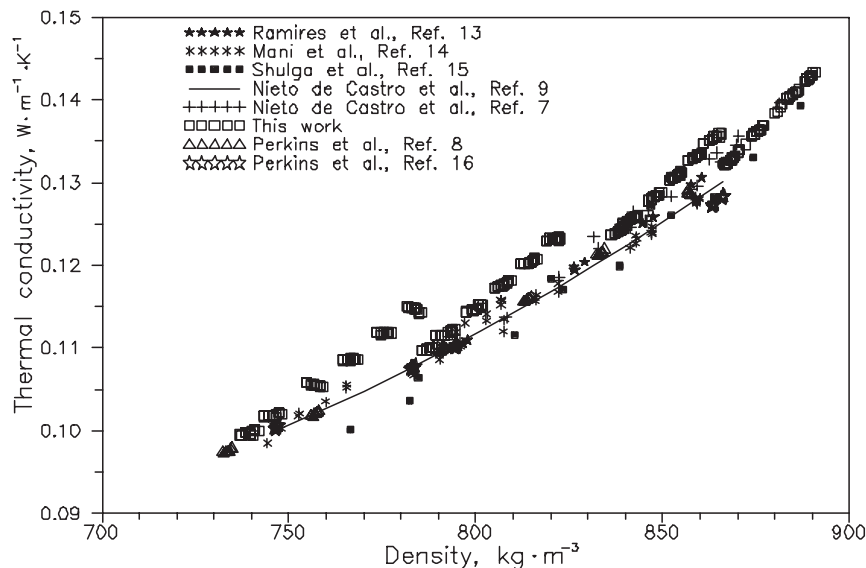


Fig. 5. Thermal conductivity of toluene as a function of density.

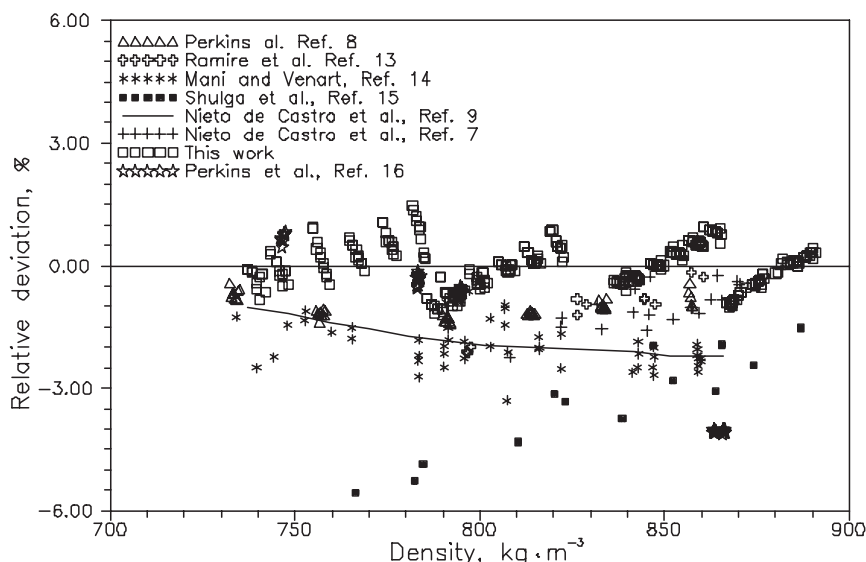


Fig. 6. Deviation in the thermal conductivity of toluene from Eq. (15).

conductivity and diffusivity using an ac-heated transient hot-wire instrument from 255 to 400 K with pressures to 1 GPa. Perkins et al. [16] measured the thermal conductivity of liquid toluene using anodized tantalum wires along the saturation line from room temperature until 550 K. In Fig. 6, it can be seen that all the thermal conductivity data, except those of Shulga et al. [15] and Perkins et al. [16], deviate at most 3% from the proposed correlation; the data of Shulga et al. deviate from Eq. (5) by -2% to -8% , the values increasing with density; the data of Perkins et al. [16] deviate from Eq. (15) by 4% at the room temperature, but deviate by less than 1% at high temperatures.

3.2.2. Thermal Diffusivity

The experimental thermal diffusivity values obtained, as well as those from the literature, are shown as a function of density in Fig. 7a. The thermal diffusivity from present work was correlated as a function of density, $735 \leq \rho \leq 870 \text{ kg} \cdot \text{m}^{-3}$, in the form

$$\alpha(\text{m}^2 \cdot \text{s}^{-1}) = [c_0 + c_1 \rho(\text{kg} \cdot \text{m}^{-3}) + c_2 (\rho(\text{kg} \cdot \text{m}^{-3}))^2] \times 10^{-8}, \quad (17)$$

with the coefficients given in Table II. Deviations of the thermal diffusivity data from all sources from that given by Eq. (17) are indicated in Fig. 8a. From this figure it can be seen that the maximum deviation for the present data set is less than 3% with a standard deviation of about 2%.

There are only three other sources of thermal diffusivity data. The data of Will et al. [17] measured along the saturation line using a optical technique, differ from -3% to -9% ; with values increasing with density. The measurements of Perkins et al. [8] diverge from the correlation by -2% to -8% , again the values increasing with density. Similarly the data of Shulga et al. [15] deviate by -1% to -9% . In the case of both Will et al. [17] and Shulga et al. [15], it is unclear what role thermal radiation has played in their measurements as no analysis was made by them of its importance. In the Perkins et al. data set [8], an analysis has been made here to correct the thermal diffusivity data to the equilibrium temperature and determine its zero time temperature offset, similar to that discussed and detailed in Appendix B. Within the mutual density range of the present measurements and those of Perkins et al. [8], zero time temperature offsets of between -8 to -23 mK were determined. Comparisons of the corrected thermal diffusivity data [8] to that of this work are shown in Figs. 7b and 8b. In the process of this correction, the temperature rise of the hot wire which have been corrected for all kinds of influences aside from the variation of the thermal conductivity and the zero temperature offset, were calculated using the thermal conductivity, thermal diffusivity, and power data

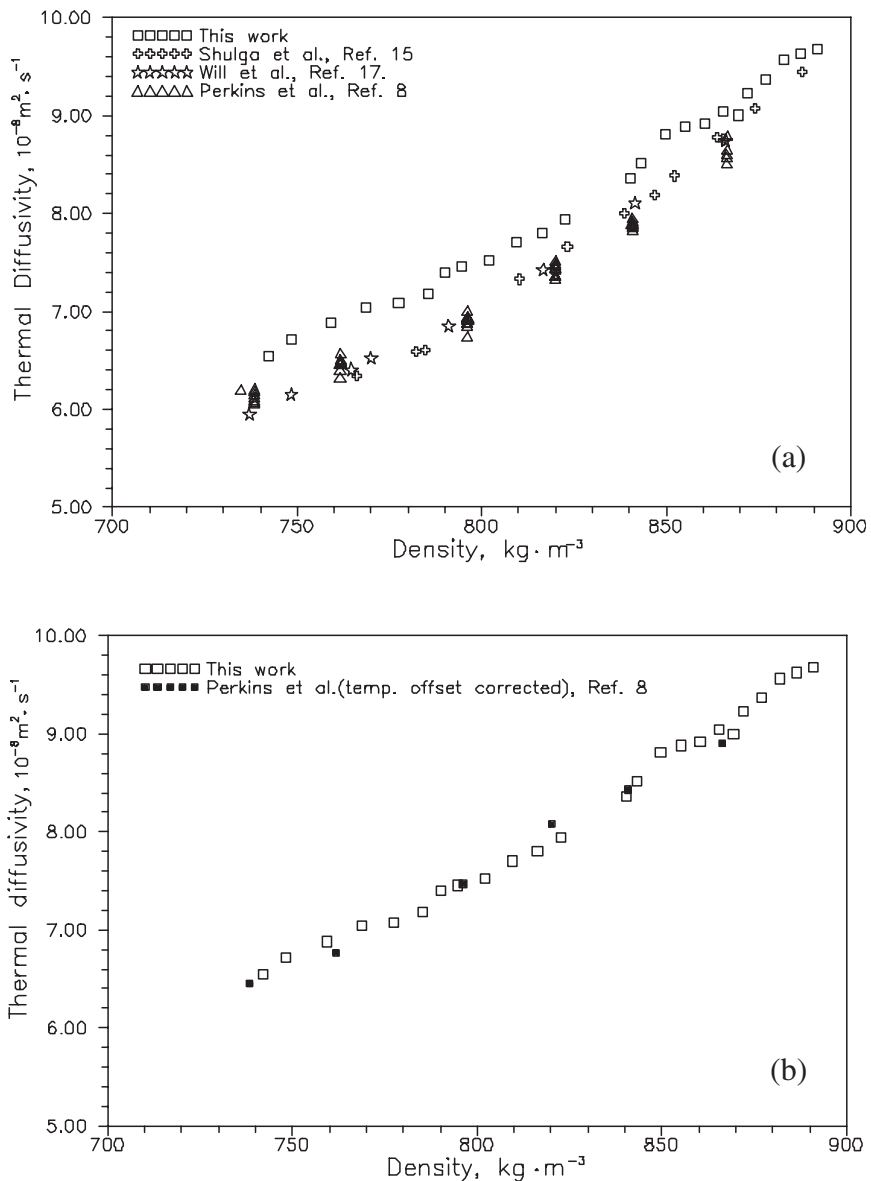


Fig. 7. Thermal diffusivity of toluene as a function of density: (a) before correcting for the temperature offset for the results in Ref. 8; (b) after correcting for the temperature offset for the results in Ref. 8 ($735 \leq \rho \leq 850 \text{ kg} \cdot \text{m}^{-3}$).

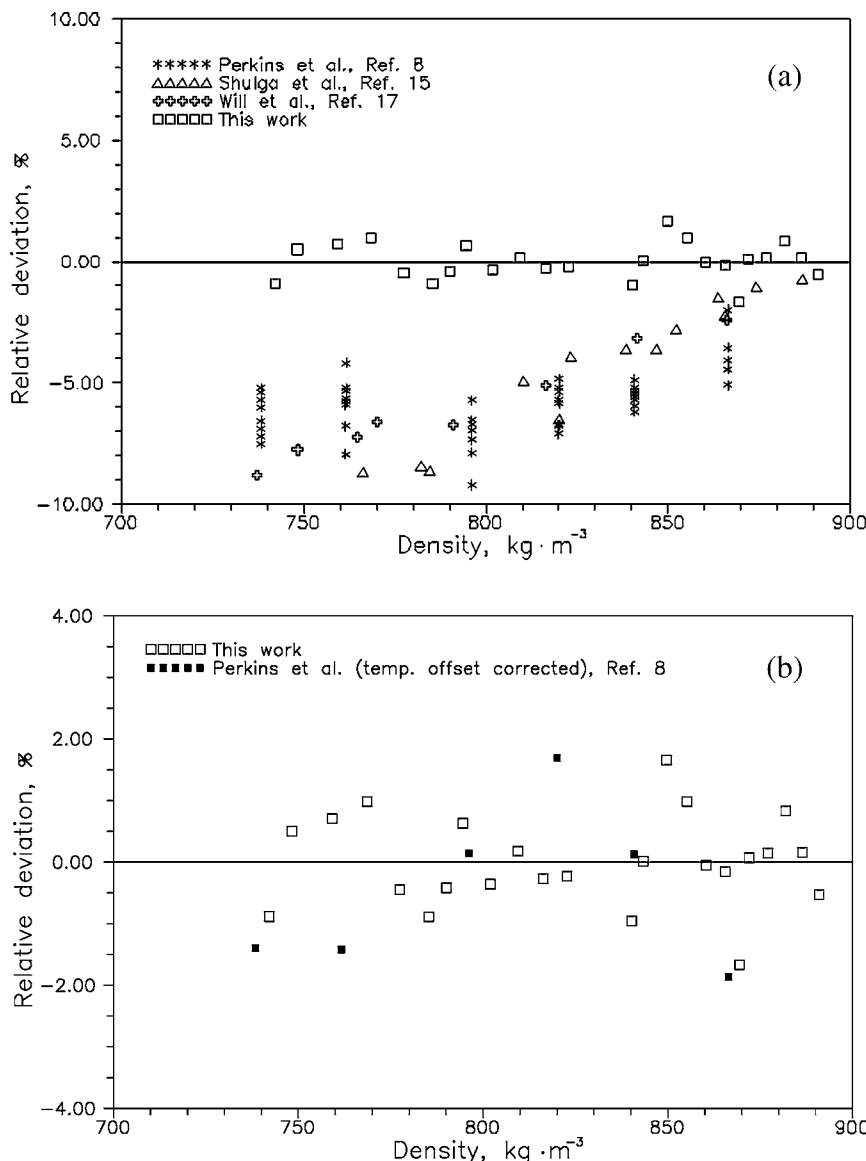


Fig. 8. Deviation of the thermal diffusivity of toluene from Eq. (17): (a) before correcting for the temperature offset for the results in Ref. 8; (b) after correcting for the temperature offset for the results in Ref. 8 ($735 \leq \rho \leq 850 \text{ kg} \cdot \text{m}^{-3}$), (this work $\pm 0.75\%$; [8] $\pm 1.43\%$ (Std. Error)).

provided in Ref. 8. From Figs. 7b and 8b it can be seen that the revised thermal diffusivity data now agree with the correlation of Eq. (17) within a standard error of less than 1.8%. However, agreement of this "corrected" data with the light scattering results of Will et al. [17] is reduced.

Figure 9 illustrates the calculated isobaric specific heat of toluene as a function of density obtained via the equation of state [11]. Figure 10 shows the relative deviations of the calculated values from those given by Ref. 11. The majority of the data deviate by less than 4%. The derived specific heat data were correlated as

$$C_p(\text{J} \cdot \text{kg}^{-1} \cdot \text{K}^{-1}) = d_0 + d_1 \rho(\text{kg} \cdot \text{m}^{-3}) + d_2(\rho(\text{kg} \cdot \text{m}^{-3}))^2 \quad (18)$$

where the coefficients are given in Table II. The deviations of the C_p data from this equation are shown in Fig. 11 where the standard deviation is less than 1.7%.

3.3. Discussion

The thermal conductivity, thermal diffusivity, and derived isobaric specific heat data given in Table IV and the derived values from the correlations given by Table II all suggest a reproducibility of better than 0.5% for thermal conductivity, 2% for thermal diffusivity, and 3% for specific

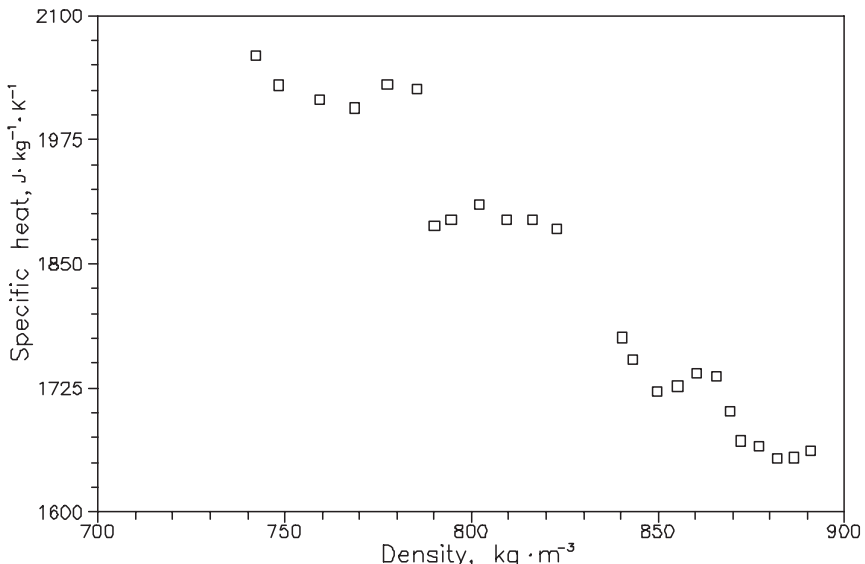


Fig. 9. Derived isobaric specific heat of toluene as a function of density.

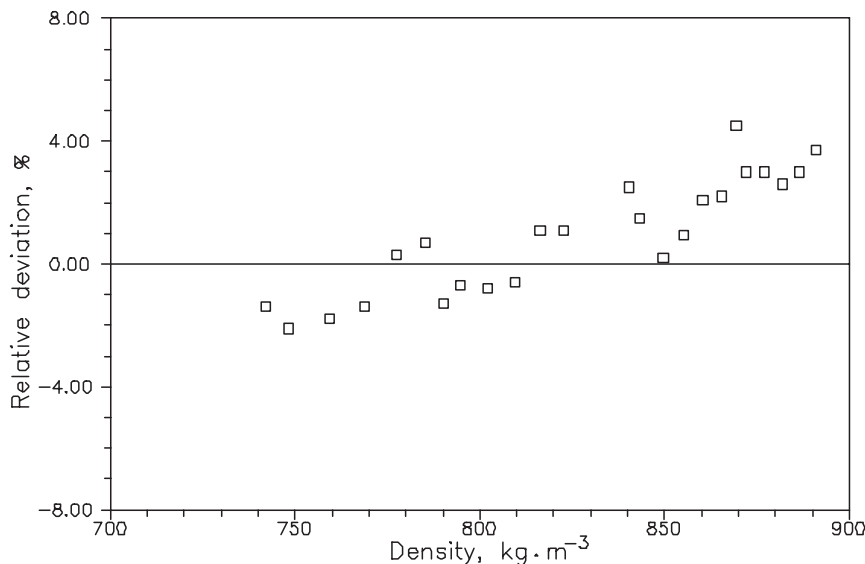


Fig. 10. Deviation in the derived isobaric specific heat of toluene from that obtained by NIST4 [11].

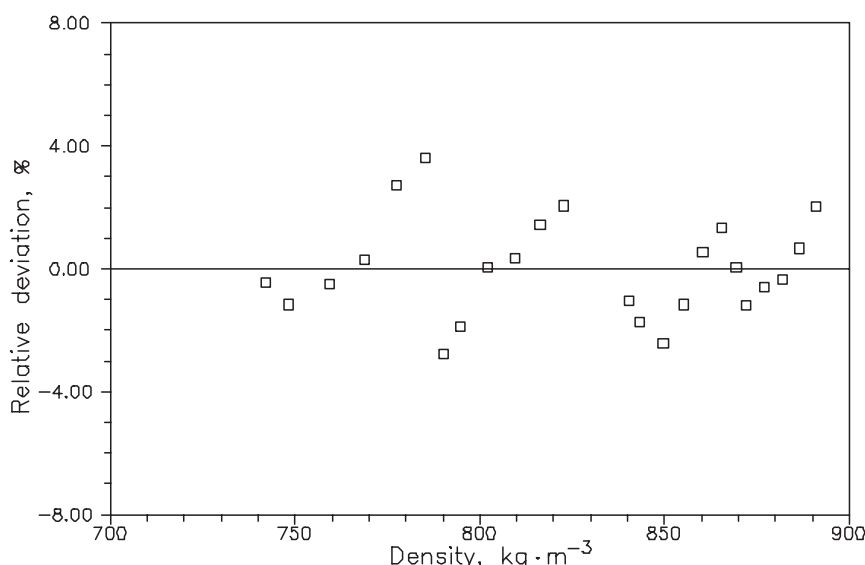


Fig. 11. Derivation in the derived isobaric specific heat of toluene from Eq. (18).

heat. The corrections for the influence of thermal radiation, wire coating, difference of hot wire diameters, bridge imbalance, and temperature variation of thermal diffusivity have all been demonstrated essential to the successful determination of thermal diffusivity, and hence the specific heat, of toluene.

It is therefore useful to examine in some detail the necessary correction procedures. As mentioned earlier, the temperature coefficient of the measured thermal conductivity near the bath temperature and at a test pressure is obtained by employing a series of powers to measure the thermal conductivity at different reference temperatures. The thermal conductivity and thermal diffusivity of the fluid corresponding to the bath temperature then result. However, a systematic and nearly constant temperature "offset" still may exist due to very small, but critical, uncertainties in the bridge and/or system balance. To obtain this correction, the temperature rise at any given instant is linearly regressed and its intercept determined (Appendix B). This correction thus represents a "zero" time effective bridge imbalance. To demonstrate the influence of this correction to measurements of thermal diffusivity, data on toluene at 324 K and 0.088 MPa for points 1201 to 1208 in the data of Ref. 8 are considered. In the process of this correction, the temperature rise of the hot wire which has been corrected for all kinds of influences aside from the variation of the thermal conductivity, and the zero temperature offset, were calculated using the thermal conductivity, thermal diffusivity and power data provided in Ref. 8. Despite a very weak dependence on density, the thermal diffusivity results, upon close examination, show a systematic variation with power; with an increase in q , values of α appear to asymptotically approach a constant, as indicated by the goodness of fit (Appendix B). The average DSTAT for the selected data sets is very much less than the DSTAT of the average of the data except when corrections are made.

For this example, the temperature coefficient of the thermal conductivity and the thermal conductivity at the thermostat equilibrium temperature can be determined; thus $\chi = -0.00219 \text{ K}^{-1}$, $\Delta T_1 = 4.0921 \text{ K}$ ($t_1 = 0.15 \text{ s}$), $\Delta T_2 = 5.2877 \text{ K}$ ($t_2 = 1.0 \text{ s}$) with $\lambda_0 = 0.1226 \text{ W} \cdot \text{m}^{-1} \cdot \text{K}^{-1}$ for a wire power, q , of $0.96177 \text{ W} \cdot \text{m}^{-1}$ (point 1201). Use of Eq. (14) returns a value of thermal diffusivity about 3.3% greater than that determined by Eq. (13) and reported in Ref. 8. Despite corrections, these adjusted results still show systematic variations in α with q (Fig. 12a); there is still an apparent increase in α with q . If the temperature rises are calculated after correcting for the influence of χ and linearly fit temperature rise vs. applied power at selected times, this will allow the determination of the "zero" time temperature offset [2-4] (Appendix B); this is $-14.67 \pm 0.17 \text{ mK}$. After correcting for this, the thermal diffusivity value obtained via Eq. (14) is

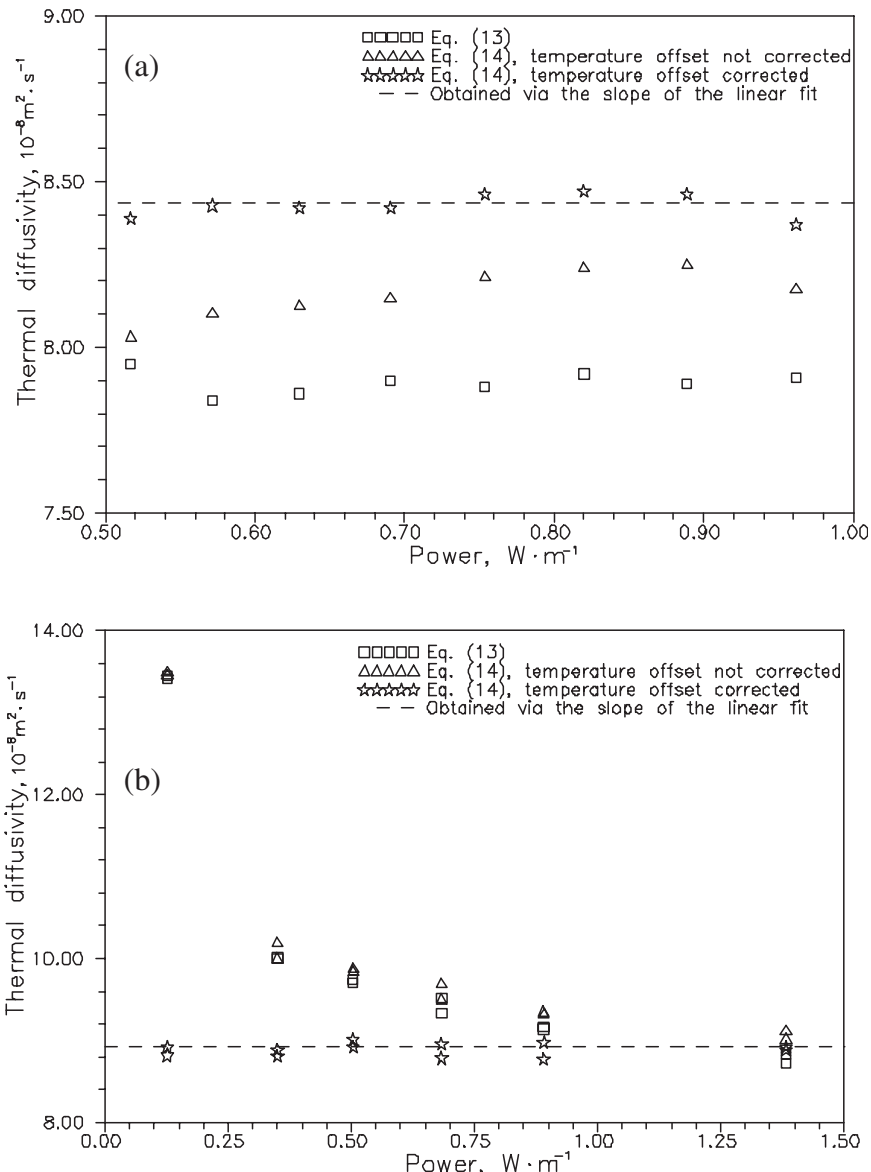


Fig. 12. Experimental thermal diffusivity of toluene before and after correcting for the influence of χ and temperature offset: (a) Ref. 8, Run ID's 1201 to 1208; (b) This work, Run ID's T50_50A3 to T50_50B8.

$8.434 \times 10^{-8} \text{ m}^2 \cdot \text{s}^{-1}$ with a DSTAT that now approaches that obtained for the average of all measurements in the set; see Fig. 12a.

Further illustration may be seen by considering data from this work, points T50_30A3 to T50_30B8 (Fig. 12b). Here again the data have been first evaluated via Eq. (13) and then corrected for the temperature variation in thermal conductivity and then again to determine the effective “zero” time temperature imbalance of the bridge of $+11.75 \pm 0.06 \text{ mK}$; this gives a thermal diffusivity of $8.914 \times 10^{-8} \text{ m}^2 \cdot \text{s}^{-1}$. Figure 13 demonstrates that the reproducibility of both sets of thermal diffusivity data are comparable and are reproducible to within $\pm 1.2\%$. Figure 14 shows the deviations in the thermal diffusivity obtained via each single measurement after correcting the influences of both χ and the temperature offset from that obtained via the slope of linear regression of the corrected temperature rise, A and $G = q/(4\pi\lambda_0)$, and it can be seen that the maximum deviation for both of the two above-mentioned examples is smaller than 2%.

The importance of this so far neglected effect emphasizes the need of very accurate bridge balances and the use of techniques, such as above, to determine equivalent “zero” time bridge imbalances in the determination of precise values of thermal diffusivity using the transient hot-wire instrument.

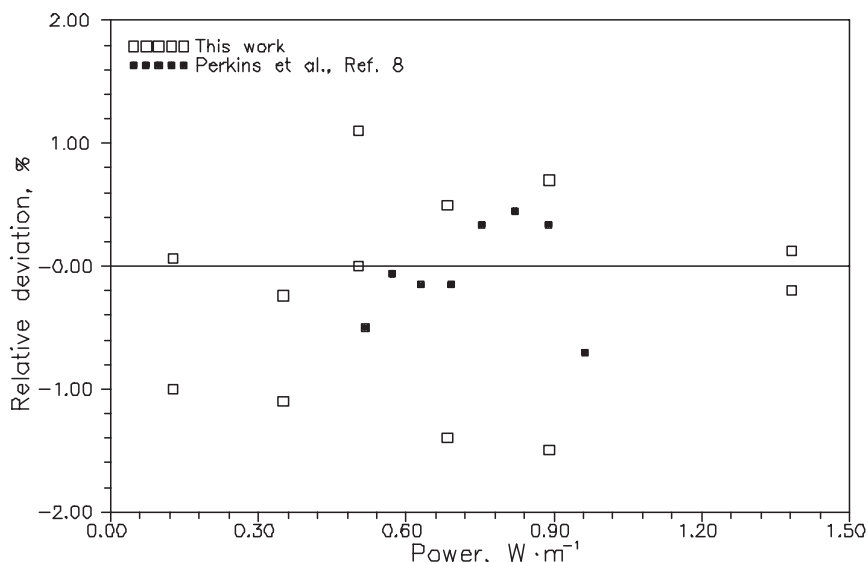


Fig. 13. Deviation in the independently determined thermal diffusivity after correcting for the influence of χ and temperature offset from that obtained via the slope of the linear regression $A \sim G$; This work, Run ID's T50_50A3 to T50_50B8; Ref. 8, Run ID's 1201 to 1208.

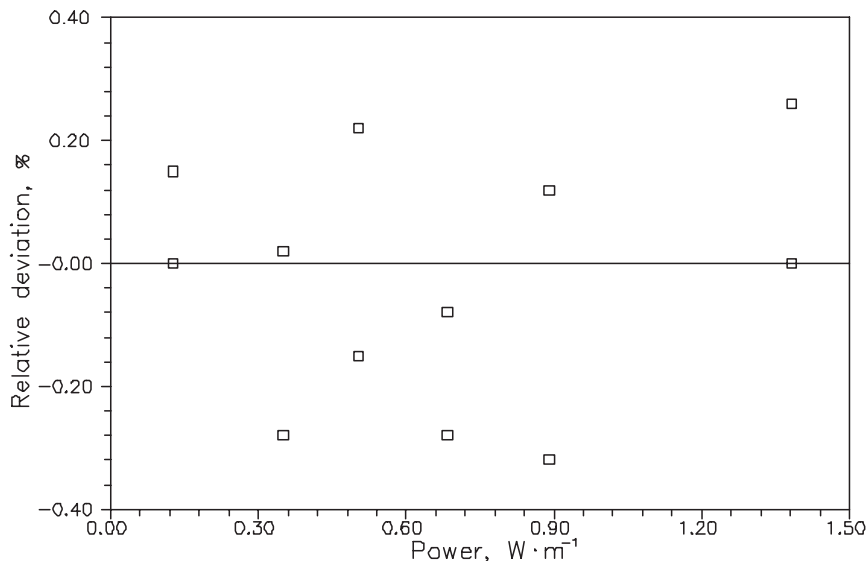


Fig. 14. Deviation in the independently determined thermal conductivity at the bath temperature obtained by correcting for the influence of χ and temperature offset from that obtained via the linear regression of $\lambda \sim \Delta T$.

Values of $\lambda(T_0, P)$ obtained using each single measurement after correcting for the influence of χ and the temperature offset are shown in Fig. 14 for the points T50_30A3 to T50_30B8. It can be seen that the thermal conductivity data deviate by less than 0.5% from the data obtained by fitting $\lambda(T_r, P)$ data vs. T_r , the reference temperature. These results indicate that the reproducibility for thermal conductivity can be secured within 0.5% and that influence of the zero time temperature offset on the thermal conductivity in the present measurements can, for all practical purposes, be ignored.

The values of B , the radiation correction parameter as a function of density are indicated in Fig. 14; B decreases with density and increases with temperature.

Additionally, from the SEM photographs of the wires and the diameter values listed in Table I, it can be seen that the uniformity of the coating is poor and that diameters, compared to those for the bare wire, may introduce considerable errors in the evaluation of the diameter of the coated wire. According to Eqs. (12) and (13), the thermal diffusivity is significantly influenced by the uncertainty of the radius of the hot wire. From

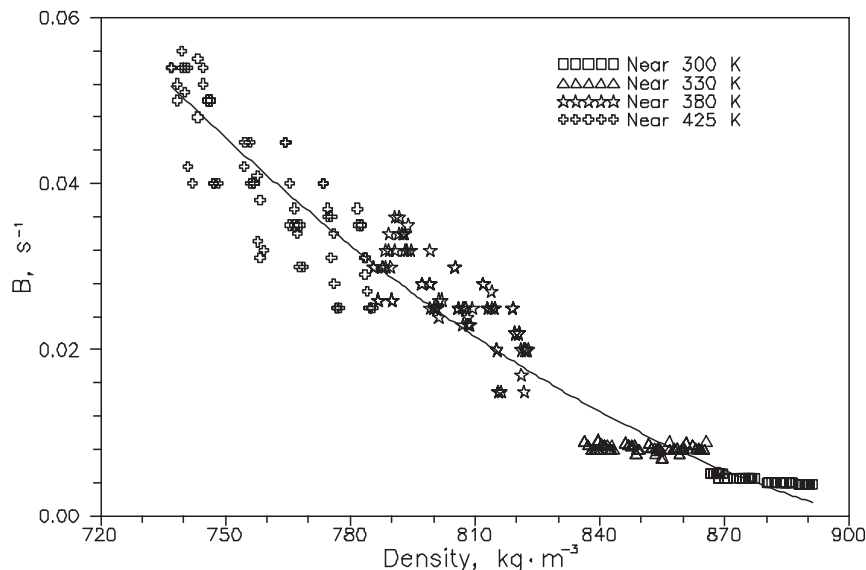


Fig. 15. Value of B of toluene as a function of density.

Eqs. (12) and (13), the relative error of the thermal diffusivity caused by the error of the hot-wire radius can be written as (Appendix A)

$$\frac{\delta\alpha}{\alpha} = \frac{2\delta a_l}{a_l} \left(1 + R_s \frac{0}{R_{l0} - R_{s0}} \right) - \frac{2\delta a_s}{a_s} \frac{R_{s0}}{R_{l0} - R_{s0}}. \quad (19)$$

From this, it can be seen that for the hot wire employed in this work, an error of 4% can be introduced if there is an error of 1% in the measured radius of the hot wire. The results for the thermal diffusivity, thermal conductivity, and specific heat of argon and toluene further indicate that the average diameters indicated in Table I for the long and short wires are sufficiently precise.

4. CONCLUSION

The thermal conductivity and thermal diffusivity of toluene in the temperature range 296 to 425 K and up to 35 MPa were measured using a transient hot-wire instrument employing coated wires. New equations for the influence of the wire coating and the thermal radiation are presented. The analysis of the influence of temperature dependent properties and residual bridge imbalance were used to obtain the thermal conductivity with an uncertainty of less than 0.5%, the thermal diffusivity with an

uncertainty of less than 2%, and derived specific heats, with an uncertainty of less than 3%.

The present measurements of thermal conductivity were employed to establish a correlation equation for the range 296 to 425 K and up to 35 MPa with an uncertainty of $\pm 2\%$. Most of the thermal conductivity data from all other data sources are in excellent agreement with this correlation with maximum uncertainties of about 3%.

The “corrected” thermal diffusivity results of Perkins et al. [8] agree well with the thermal diffusivity values obtained in this work within the range of mutual uncertainty, but more poorly with dynamic light scattering measurements of Will et al. [17] where there should be no thermal radiation correction since there is no temperature gradient imposed during the measurement.

APPENDIX A: INFLUENCE OF A COATED WIRE AND WIRE DIAMETER VARIATION

For wires with coatings, if end effects are ignored, the energy equation is

$$\frac{\partial^2 \Delta T_1}{\partial r^2} + \frac{1}{r} \frac{\partial \Delta T_1}{\partial r} - \frac{1}{\alpha_1} \frac{\partial \Delta T_1}{\partial t} = -\frac{q}{\pi a_1^2 \lambda_1}, \quad (\text{A1})$$

$$\frac{\partial^2 \Delta T_2}{\partial r^2} + \frac{1}{r} \frac{\partial \Delta T_2}{\partial r} - \frac{1}{\alpha_2} \frac{\partial \Delta T_2}{\partial t} = 0, \quad (\text{A2})$$

$$\frac{\partial^2 \Delta T_3}{\partial r^2} + \frac{1}{r} \frac{\partial \Delta T_3}{\partial r} - \frac{1}{\alpha_3} \frac{\partial \Delta T_3}{\partial t} = 0, \quad (\text{A3})$$

with the corresponding boundary and initial conditions

$$r = 0, \quad \frac{\partial \Delta T_1}{\partial r} = 0, \quad (\text{A4})$$

$$r = a_1, \quad \Delta T_1 = \Delta T_2, \quad \lambda_1 \frac{\partial \Delta T_1}{\partial r} = \lambda_2 \frac{\partial \Delta T_2}{\partial r}, \quad (\text{A5})$$

$$r = a_2, \quad \Delta T_2 = \Delta T_3, \quad \lambda_2 \frac{\partial \Delta T_2}{\partial r} = \lambda_3 \frac{\partial \Delta T_3}{\partial r}, \quad (\text{A6})$$

$$r \rightarrow \infty, \quad \Delta T_3 = 0, \quad \text{and} \quad (\text{A7})$$

$$t = 0, \quad \Delta T_1 = \Delta T_2 = \Delta T_3 = 0, \quad (\text{A8})$$

where a_1 and a_2 are the radii of the bare and coated wires, respectively; λ and α are the thermal conductivity and thermal diffusivity, respectively; and the subscripts 1, 2, and 3 represent the wire, the coating, and the test fluid, respectively; q is the energy input per unit length of wire.

After Laplace transformation, the equations can be expressed as

$$\frac{\partial^2 \Delta\bar{T}_1}{\partial r^2} + \frac{1}{r} \frac{\partial \Delta\bar{T}_1}{\partial r} - \frac{p}{\alpha_1} \Delta\bar{T}_1 = -\frac{q}{p\pi a_1^2 \lambda_1}, \quad (\text{A9})$$

$$\frac{\partial^2 \Delta\bar{T}_2}{\partial r^2} + \frac{1}{r} \frac{\partial \Delta\bar{T}_2}{\partial r} - \frac{p}{\alpha_2} \Delta\bar{T}_2 = 0, \quad (\text{A10})$$

$$\frac{\partial^2 \Delta\bar{T}_3}{\partial r^2} + \frac{1}{r} \frac{\partial \Delta\bar{T}_3}{\partial r} - \frac{p}{\alpha_3} \Delta\bar{T}_3 = 0, \quad (\text{A11})$$

with the boundary and initial conditions,

$$r = 0, \quad \frac{\partial \Delta\bar{T}_1}{\partial r} = 0, \quad (\text{A12})$$

$$r = a_1, \quad \Delta\bar{T}_1 = \Delta\bar{T}_2, \quad \lambda_1 \frac{\partial \Delta\bar{T}_1}{\partial r} = \lambda_2 \frac{\partial \Delta\bar{T}_2}{\partial r}, \quad (\text{A13})$$

$$r = a_2, \quad \Delta\bar{T}_2 = \Delta\bar{T}_3, \quad \lambda_2 \frac{\partial \Delta\bar{T}_2}{\partial r} = \lambda_3 \frac{\partial \Delta\bar{T}_3}{\partial r}, \quad (\text{A14})$$

$$r \rightarrow \infty, \quad \Delta\bar{T}_3 = 0, \quad (\text{A15})$$

where p is the Laplace transformation variable.

The general solutions for $\Delta\bar{T}_1$, $\Delta\bar{T}_2$, and $\Delta\bar{T}_3$ are

$$\Delta\bar{T}_1 = c_1 I_0(q_1 r) + c_2 K_0(q_1 r) - G, \quad (\text{A16})$$

$$\Delta\bar{T}_2 = d_1 I_0(q_2 r) + d_2 K_0(q_2 r), \quad (\text{A17})$$

$$\Delta\bar{T}_3 = e_1 I_0(q_3 r) + e_2 K_0(q_3 r), \quad (\text{A18})$$

where $q_1 = \sqrt{p/\alpha_1}$, $q_2 = \sqrt{p/\alpha_2}$, and $q_3 = \sqrt{p/\alpha_3}$. I and K are Bessel functions of second class.

For boundary conditions at $r = 0$, $r \rightarrow \infty$; $c_2 = 0$ and $e_2 = 0$, with the continuity equation at $r = a_1$, $r = a_2$, we obtain

$$c_1 I_0(q_1 a_1) - G = d_1 I_0(q_2 a_1) + d_2 K_0(q_2 a_1), \quad (\text{A19})$$

$$d_1 I_0(q_2 a_2) + d_2 K_0(q_2 a_2) = e_3 K_0(q_3 a_2), \quad (\text{A20})$$

$$c_1 q_1 I_1(q_1 a_1) = d_2 \lambda_2 q_2 I_1(q_2 a_1) - d_2 \lambda_2 q_2 K_1(q_2 a_1), \quad (\text{A21})$$

$$d_1 \lambda_2 q_2 I_1(q_2 a_2) - d_2 \lambda_2 q_2 K_1(q_2 a_2) = -e_2 \lambda_3 q_3 K_1(q_3 a_2). \quad (\text{A22})$$

From these, the ratio of d_1 to d_2 can be written as

$$\frac{d_1}{d_2} = \frac{\lambda_2 q_2 K_0(q_3 a_2) K_1(q_2 a_2) - \lambda_3 q_3 K_1(q_3 a_2) K_0(q_2 a_2)}{\lambda_3 q_3 K_1(q_3 a_2) I_0(q_3 a_2) + \lambda_2 q_2 K_0(q_3 a_2) I_1(q_2 a_2)}. \quad (\text{A23})$$

The numerator of d_2 , n_2 , is

$$n_2 = \lambda_3 q_3 K_1(q_3 a_2) I_0(q_2 a_2) + \lambda_2 q_2 K_0(q_3 a_2) I_1(q_2 a_2). \quad (\text{A24})$$

The numerator of d_1 , n_1 , is

$$n_1 = \lambda_2 q_2 K_0(q_3 a_2) K_1(q_2 a_2) - \lambda_3 q_3 K_0(q_2 a_2) K_1(q_3 a_2). \quad (\text{A25})$$

The denominator of d_1 and d_2 , D , is

$$\begin{aligned} D = & [\lambda_2 q_2 K_0(q_3 a_2) K_1(q_2 a_2) - \lambda_3 q_3 K_1(q_3 a_2) K_0(q_2 a_2)] \\ & \times [\lambda_2 q_2 I_0(q_1 a_1) I_1(q_2 a_1) - \lambda_1 q_1 I_1(q_1 a_1) I_0(q_2 a_1)] \\ & - [\lambda_2 q_2 I_0(q_1 a_1) K_1(q_2 a_1) + \lambda_1 q_1 I_1(q_1 a_1) K_0(q_2 a_1)] \\ & \times [\lambda_3 q_3 K_1(q_3 a_2) I_0(q_2 a_2) + \lambda_2 q_2 K_0(q_3 a_2) I_1(q_2 a_2)]. \end{aligned} \quad (\text{A26})$$

Using the approximate form of the Bessel Functions; n_1 , n_2 and D can be expressed as,

$$\begin{aligned} n_1 = & \frac{G \lambda_1 q_1^2 a_1}{2 a_2} \left[\lambda_2 \ln \frac{C q_3 a_2}{2} + \frac{\lambda_2 q_3^2 a_2^2}{4} \left(\ln \frac{C q_3 a_2}{2} - 1 \right) \right. \\ & - \lambda_3 \ln \frac{C q_2 a_2}{2} - \frac{\lambda_3 q_2^2 a_2^2}{4} \left(\ln \frac{C q_2 a_2}{2} - 1 \right) \\ & \left. + \frac{\lambda_2 q_2^2 a_2^2}{2} \ln \frac{C q_3 a_2}{2} \left(\ln \frac{C q_2 a_2}{2} - \frac{1}{2} \right) - \frac{\lambda_3 q_3^2 a_2^2}{2} \ln \frac{C q_2 a_2}{2} \left(\ln \frac{C q_3 a_2}{2} - \frac{1}{2} \right) \right] \end{aligned} \quad (\text{A27})$$

$$n_2 = \frac{G \lambda_1 q_1^2 a_1}{2 a_2} \left[\frac{\lambda_2 q_2^2 a_2^2}{2} \ln \frac{C q_3 a_2}{2} - \lambda_3 - \frac{\lambda_3 q_2^2 a_2^2}{4} - \frac{\lambda_3 q_3^2 a_2^2}{2} \left(\ln \frac{C q_3 a_2}{2} - \frac{1}{2} \right) \right] \quad (\text{A28})$$

$$\frac{1}{D} = -\frac{a_1 a_2}{\lambda_2 \lambda_3} \left[1 - \frac{q_3^2 a_2^2}{2} \left(\ln \frac{C q_3 a_2}{2} - \frac{1}{2} \right) - \frac{q_2^2 a_2^2}{4} - \frac{q_1^2 a_1^2}{4} + \frac{q_2^2 a_1^2}{4} + \frac{q_2^2 a_1^2}{2} \ln \frac{a_2}{a_1} \right. \\ \left. + \frac{\lambda_2 q_2^2 (a_2^2 - a_1^2)}{2 \lambda_3} \ln \frac{C q_3 a_2}{2} + \frac{q_1^2 a_1^2}{2} \ln \frac{a_1}{a_2} + \frac{\lambda_1 q_1^2 a_1^2}{2 \lambda_3} \ln \frac{C q_3 a_2}{2} \right], \quad (\text{A29})$$

$$c_1 = \frac{d_1 I_0(q_2 a_1)}{I_0(q_1 a_1)} + \frac{d_2 K_0(q_2 a_1)}{I_0(q_1 a_1)} - \frac{G}{I_0(q_1 a_1)}, \quad (\text{A30})$$

$$e_2 = \frac{d_1 I_0(q_2 a_2) + d_2 K_0(q_2 a_2)}{K_0(q_3 a_2)}. \quad (\text{A31})$$

Approximate solutions for ΔT_1 , ΔT_2 , and ΔT_3 can then be obtained [18], and the inverse Laplace transformations of ΔT_1 , ΔT_2 , and ΔT_3 , i.e., the temperature rise of the hot wire, the coating, and the test fluid,

$$\Delta T_1(r, t) = \frac{q}{4\pi\lambda_3} \left[\ln \frac{4\alpha_3 t}{a_2^2 C} + \frac{2\lambda_3}{\lambda_2} \ln \frac{a_2}{a_1} + \frac{a_1^2}{2\lambda_3 t} \left(\frac{\lambda_2}{\alpha_2} - \frac{\lambda_1}{\alpha_1} \right) \ln \frac{4\alpha_3 t}{a_2^2 C} \right. \\ \left. + \frac{a_2^2}{2\lambda_3 t} \left(\frac{\lambda_3}{\alpha_3} - \frac{\lambda_2}{\alpha_2} \right) \ln \frac{4\alpha_3 t}{a_2^2 C} + \left(\frac{a_1^2}{\alpha_2 t} - \frac{a_1^2}{\alpha_1 t} \right) \ln \frac{a_2}{a_1} \right. \\ \left. + \frac{1}{2} \left(\frac{a_1^2 - a_2^2}{\alpha_2 t} + \frac{a_2^2}{\alpha_3 t} - \frac{a_1^2}{\alpha_1 t} + \frac{r^2}{2\alpha_1 t} \right) - \frac{\lambda_3(r^2 - a^2)}{\lambda_1 a_1^2} \right], \quad (\text{A32})$$

$$\Delta T_2(r, t) = \frac{q}{4\pi\lambda_3} \left[\ln \frac{4\alpha_3 t}{a_2^2 C} + \frac{a_1^2}{2\lambda_3 t} \left(\frac{\lambda_2}{\alpha_2} - \frac{\lambda_1}{\alpha_1} \right) \ln \frac{4\alpha_3 t}{a_2^2 C} + \frac{a_2^2}{2\lambda_3 t} \left(\frac{\lambda_3}{\alpha_3} - \frac{\lambda_2}{\alpha_2} \right) \ln \frac{4\alpha_3 t}{a_2^2 C} \right. \\ \left. + \frac{a_2^2}{2\alpha_3 t} - \frac{a_1^2}{4\alpha_1 t} - \frac{a_2^2}{2\alpha_2 t} + \frac{a_1^2}{4\alpha_2 t} + \frac{r^2}{4\alpha_2 t} \right. \\ \left. + \frac{a_1^2}{2t} \left(\frac{1}{\alpha_2} - \frac{1}{\alpha_1} \right) \ln \frac{a_2^2}{a_1 r} + \frac{2\lambda_3}{\lambda_2} \ln \frac{a_2}{a_1} \right], \quad (\text{A33})$$

$$\Delta T_3(r, t) = \frac{q}{4\pi\lambda_3} \left[\ln \frac{4\alpha_3 t}{a^2 C} - \frac{1}{2\lambda_3 t} \left(\frac{\lambda_1 a_1^2}{\alpha_1} + \frac{\lambda_2 a_2^2}{\alpha_2} - \frac{\lambda_2 a_1^2}{\alpha_2} + \frac{\lambda_3 a_2^2}{\alpha_3} \right) \ln \frac{4\alpha_3 t}{r^2 C} \right. \\ \left. + \frac{2\lambda_3}{\lambda_2} \ln \frac{a_2}{a_1} + \frac{a_2^2}{2\alpha_3 t} - \frac{a_1^2}{4\alpha_1 t} - \frac{a_2^2}{2\alpha_2 t} + \frac{a_1^2}{4\alpha_2 t} + \frac{r^2}{4\alpha_2 t} \right. \\ \left. + \frac{1}{2\lambda_3 t} \left(\frac{a_1^2}{2\alpha_2 t} - \frac{a_1^2}{2\alpha_1 t} \right) \ln \frac{a_2}{a_1} \right. \\ \left. + \frac{1}{2\lambda_3 t} \left(\frac{\lambda_1 a_1^2}{\alpha_2} + \frac{\lambda_2 a_2^2}{\alpha_2} - \frac{\lambda_2 a_1^2}{\alpha_2} + \frac{\lambda_3 a_2^2}{\alpha_3} \right) \ln \frac{a_2}{r} \right] \quad (\text{A34})$$

Table AI. Thermal Conductivity and Thermal Diffusivity Values Assuming Both the Wires Have Radius Value of the Long Wire for Run ID's T50_50A3 to T50_50B8

Tr_r (K)	q (W·m ⁻¹)	A_1 (W·m ⁻¹ ·K ⁻¹)	$\alpha_1 \times 10^8$ (m ² ·s ⁻¹)	T_r (K)	λ_2 (W·m ⁻¹ ·K ⁻¹)	$\alpha_2 \times 10^8$ (m ² ·s ⁻¹)
327.630		0.1362	8.914	327.63	0.1353	8.421
328.190	0.12652	0.1361	13.587	328.18	0.1353	12.845
328.193	0.12647	0.1360	13.540	328.19	0.1351	12.521
329.161	0.35025	0.1358	10.157	329.15	0.1350	9.375
329.162	0.35023	0.1358	10.007	329.15	0.1350	9.292
329.830	0.50348	0.1357	9.7726	329.81	0.1349	9.018
329.833	0.50351	0.1357	9.8028	329.81	0.1349	9.046
330.654	0.68352	0.1355	9.5845	330.59	0.1347	8.849
330.661	0.68356	0.1355	9.3950	330.58	0.1347	8.673
331.494	0.89054	0.1353	9.2165	331.47	0.1345	8.512
331.497	0.89037	0.1353	9.2339	331.48	0.1345	8.528
333.600	1.38239	0.1348	8.8022	333.58	0.1340	8.132
333.611	1.38247	0.1348	8.9051	333.59	0.1340	8.227

The difference between Eq. (A32) and the result given in Ref. 1 is

$$\frac{q}{4\pi\lambda_3} \times \frac{r^2 - a^2}{4\lambda_1} \left[(\lambda_2 - \lambda_3) \left(\frac{1}{\alpha_1 t} - \frac{1}{\alpha_2 t} \right) + \frac{\lambda_1}{\alpha_1 t} \right]$$

If we average across the diameter, this can be written as

$$-\frac{q}{4\pi\lambda_3} \times \frac{a^2}{8\lambda_1} \left[(\lambda_2 - \lambda_3) \left(\frac{1}{\alpha_1 t} - \frac{1}{\alpha_2 t} \right) + \frac{\lambda_1}{\alpha_1 t} \right].$$

In the current measurements for toluene, this difference is smaller than 0.1 mK and the error introduced to the thermal conductivity and thermal diffusivity cannot be detected.

The influence in differences in the size of wire diameter are illustrated in Table AI.

APPENDIX B: DETERMINATION OF THERMAL DIFFUSIVITY

B.1. Thermal Diffusivity

In order to obtain accurate thermal diffusivity values, the following steps must be taken:

- For each power level q , use experimental λ and α values obtained at T_r and T_0 to calculate the ideal temperature rise of the hot wire, ΔT , for selected times, say $t = 250, 500, 750$, and 1000 ms.
- Linearly correlate the set of λ versus T_r to obtain λ_0 and its temperature coefficient, χ .
- Use χ to obtain the corrected temperature rise of the hot wire, A

$$A = \Delta T + \frac{1}{2} \chi \Delta T^2. \quad (\text{B1})$$

- Calculate $G = q/4\pi\lambda_0$ using appropriate values of q and λ_0 .
- Correlate A vs G . The slope of this linear regression is $\ln(4\alpha_0 t/a^2 C)$, and the A intercept is the temperature offset δT_{00} due to the 'zero' time bridge or system unbalance.
- Re-correct the temperature rise of the hot wire A'

$$A' = \Delta T + \delta T_{00}. \quad (\text{B2})$$

- Correlate A' vs G to determine α'_0 .

The following examples are taken from corrections to Ref. 8 data. Measurement example 1 for toluene by Perkins et al. [8] at 401.3 K, Run

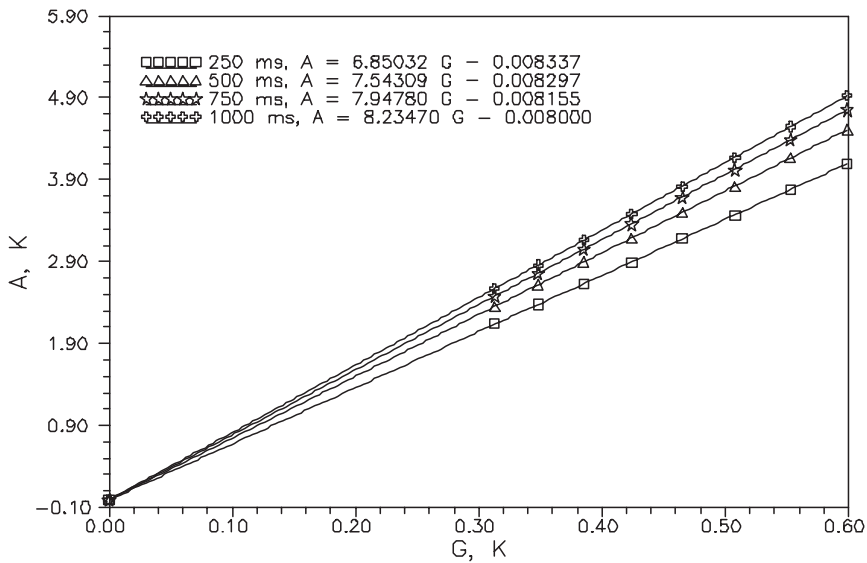


Fig. B1. Calculated temperature rise at different times as a function of power after correcting for the influence of χ ; Ref. 8, Run ID's 1501 to 1508: determined temperature offset $= -8.2 \pm 0.2$ mK.

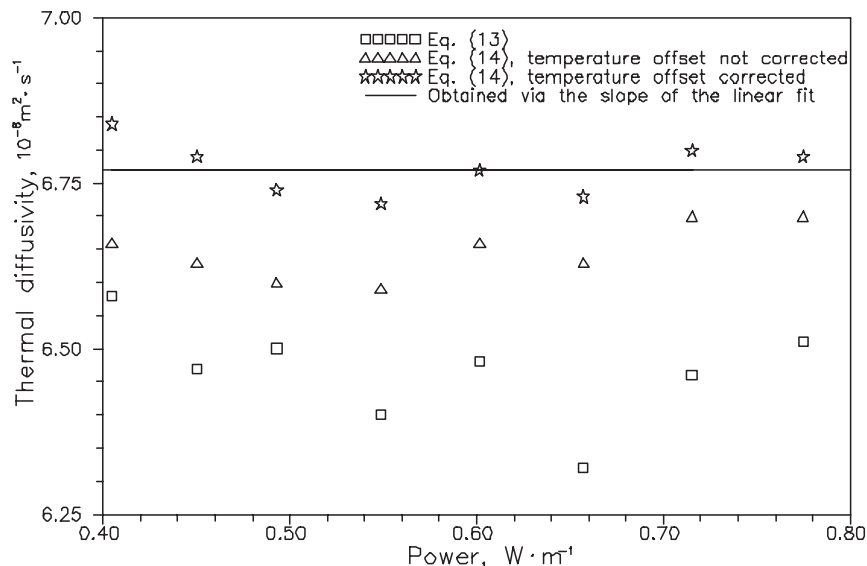


Fig. B2. Thermal diffusivity before and after correcting for the influence of χ and temperature offset; Ref. 8, Run ID's 1501 to 1508: $\alpha'_0 = 6.772 \pm 0.041 \times 10^{-8} \text{ m}^2 \cdot \text{s}^{-1}$.

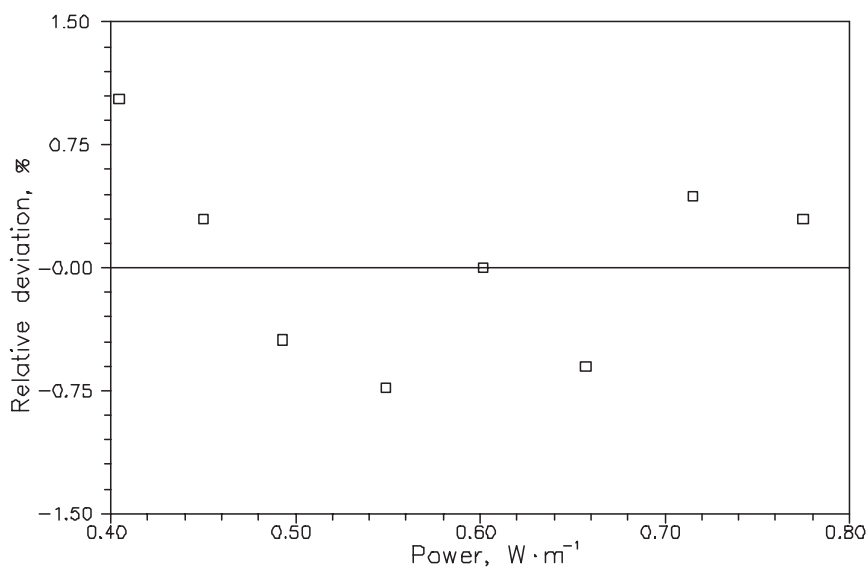


Fig. B3. Deviation in the independently determined thermal diffusivity after correcting for the influence of χ and temperature offset from that obtained via the slope of the linear regression A ~ G; Ref. 8, Run ID's 1501 to 1508.

ID's 1501 to 1508; the determined temperature coefficient of thermal conductivity, $\chi = -0.002560$; the temperature offset $\delta T_{0^\circ} = -8.2 \pm 0.2$ mK, $\lambda_0 = 0.10294 \text{ W} \cdot \text{m}^{-1}$; and $\alpha'_0 = 6.772 \pm 0.0406 \times 10^{-8} \text{ m}^2 \cdot \text{s}^{-1}$. The linear regression of A versus G, the thermal diffusivity after different corrections at different powers, and the deviation in the independently determined thermal diffusivity after correcting for the influence of χ and temperature offset from that obtained via the slope of the linear regression A vs. G are shown in Figs. B1–B3.

The change in average thermal diffusivity value with χ correction is $+2.8\%$ and with both χ and δT_{0° is $+4.75\%$.

Measurement example 2 for toluene by Perkins et al. [8] at 422.5 K, Run ID's 1601 to 1608; the temperature coefficient of thermal conductivity, $\chi = -0.002148$; the temperature offset, δT_{0° , is -13.9 ± 0.4 mK, $\lambda_0 = 0.098309 \text{ W} \cdot \text{m}^{-1}$, and $\alpha'_0 = 6.449 \pm 0.022 \times 10^{-8} \text{ m}^2 \cdot \text{s}^{-1}$. The linear regression of A versus G, thermal diffusivity after different corrections at different powers, and the deviation in the independently determined thermal diffusivity after correcting for the influence of χ and temperature offset from that obtained via the slope of the linear regression A vs G are shown in Figs. B4 to B6.

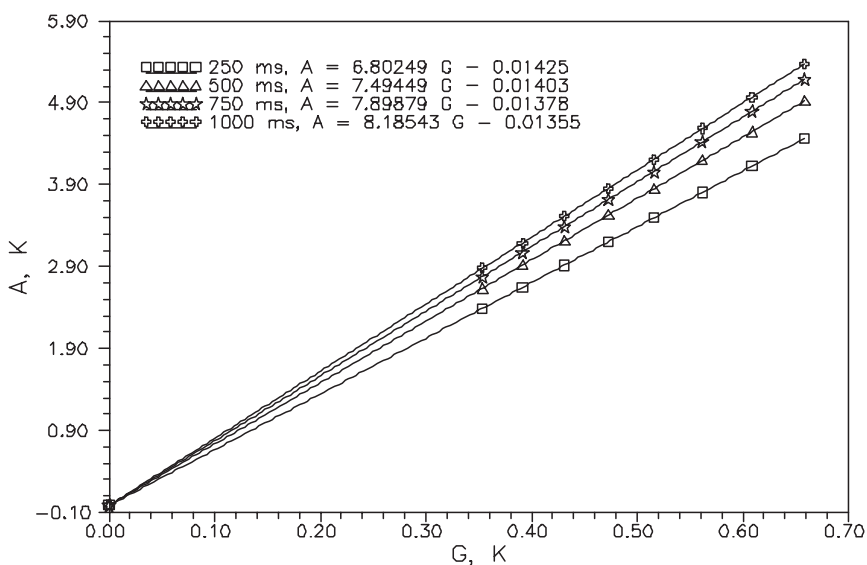


Fig. B4. Calculated temperature rise at different times as a function of power after correcting for the influence of χ ; Ref. 8, Run ID's 1601 to 1608: determined temperature offset $= -13.9 \pm 0.4$ mK.

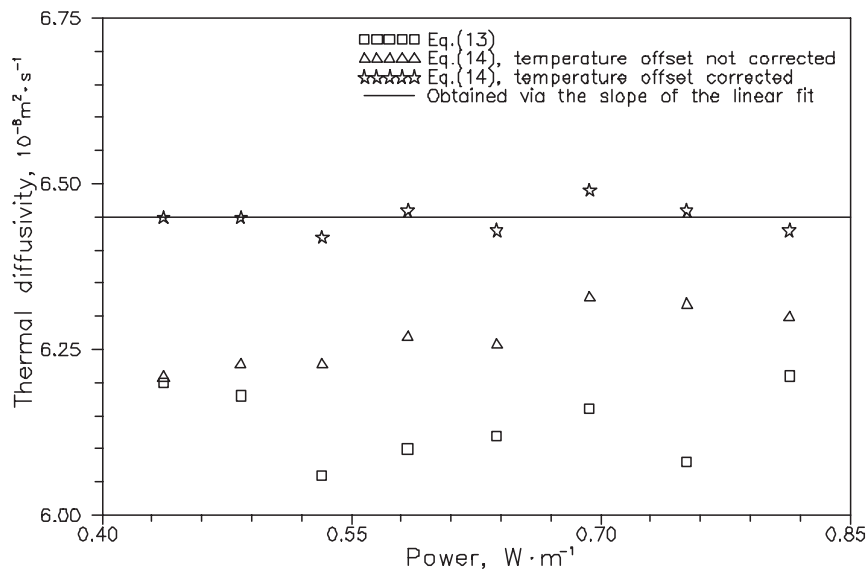


Fig. B5. Thermal diffusivity before and after correcting for the influence of χ and temperature offset; Ref. 8, Run ID's 1501 to 1508 $\alpha'_0 = 6.449 \pm 0.022 \times 10^{-8} \text{ m}^2 \cdot \text{s}^{-1}$.

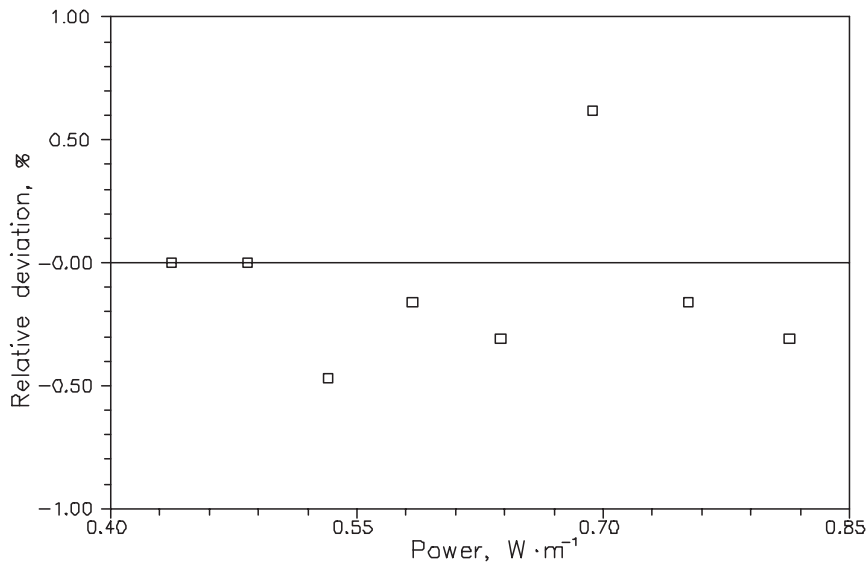


Fig. B6. Deviation in the independently determined thermal diffusivity after correcting for the influence of χ and temperature offset from that obtained via the slope of the linear regression A ~ G; Ref. 8, Run ID's 1601 to 1608.

The change in average thermal diffusivity value with χ correction is +2.1% and with both χ and δT_0 is +5.05%.

B.2. The Influence of Bath Temperature Variation on Thermal Diffusivity

Suppose two measurements at powers, q_1 and q_2 , are utilized to obtain the thermal conductivities λ_1 and λ_2 at the reference temperatures T_1 and T_2 . From these two results the thermal conductivity, λ_0 , the temperature coefficient of thermal conductivity, χ , as well as the thermal diffusivity α at the mean bath temperature T_0 can be determined. If the difference in bath temperature is δT_1 for the measurement at q_1 and δT_2 of for the measurement at q_2 , the temperature rises, corresponding to λ_1 and λ_2 , are ΔT_1 and ΔT_2 and

$$\lambda_1 = \lambda_0(1 + \chi \Delta T_1), \quad (\text{B3})$$

$$\lambda_2 = \lambda_0(1 + \chi \Delta T_2). \quad (\text{B4})$$

Then λ_0 and χ can be obtained from

$$\lambda_0 = \frac{\lambda_1 \Delta T_2 - \lambda_2 \Delta T_1}{\Delta T_2 - \Delta T_1}, \quad (\text{B5})$$

$$\chi = \frac{\lambda_1 - \lambda_2}{\lambda_2 \Delta T_1 - \lambda_1 \Delta T_2}. \quad (\text{B6})$$

Thus, the error introduced in λ_0 and χ , due to a discrepancy in T_0 for the two measurements, can be stated as

$$\delta \lambda_0 = -\frac{\lambda_1 \Delta T_2 - \lambda_2 \Delta T_1}{(\Delta T_2 - \Delta T_1)^2} (\delta T_2 - \delta T_1) + \frac{\lambda_1 \delta T_2 + \Delta T_2 \delta \lambda_1 - \lambda_2 \delta T_1 - \Delta T_1 \delta \lambda_2}{\Delta T_2 - \Delta T_1}, \quad (\text{B7})$$

and

$$\delta \chi = -\frac{(\lambda_1 - \lambda_2)(\lambda_2 \delta T_1 - \lambda_1 \delta T_2 + \Delta T_1 \delta \lambda_2 - \Delta T_2 \delta \lambda_1)}{(\lambda_2 \Delta T_1 - \lambda_1 \Delta T_2)^2} + \frac{\delta \lambda_1 - \delta \lambda_2}{\lambda_2 \Delta T_1 - \lambda_1 \Delta T_2}. \quad (\text{B8})$$

Usually the thermal conductivity can be expressed as a function of density and temperature, i.e.,

$$\lambda = a_2 T^2 + a_1 T + a_0 + b_2 \rho^2 + b_1 \rho + b_0, \quad (\text{B9})$$

and hence the departure, $\delta\lambda_1$ and $\delta\lambda_2$, caused by deviations from T_0 , can be written as

$$\delta\lambda_1 = (2a_2T + a_1)\delta T_1 + (2b_2\rho + b_1)\delta\rho_1, \quad (\text{B10})$$

$$\delta\lambda_2 = (2a_2T + a_1)\delta T_2 + (2b_2\rho + b_1)\delta\rho_2. \quad (\text{B11})$$

If there is no difference in T_0 , the temperature rise of the hot wire is

$$\Delta T = \frac{q}{4\pi\lambda_0(1+\chi\Delta T_r)} \ln \frac{4\alpha t}{a^2 C}, \quad (\text{B12})$$

where ΔT_r denotes the temperature difference between T_r and T_0 . If the discrepancy in bath temperature, δT , is taken into account, Eq. (B12) becomes

$$\Delta T' = \frac{q}{4\pi\lambda_0[1+\chi(\Delta T_r + \delta T)]} \ln \frac{4\alpha t}{a^2 C}, \quad (\text{B13})$$

and the error in ΔT caused by δT in the two measurements at q_1 and q_2 is

$$\delta T_{r1} = -\frac{\delta\lambda_1}{\lambda_1} \Delta T_1, \quad (\text{B14})$$

$$\delta T_{r2} = -\frac{\delta\lambda_2}{\lambda_2} \Delta T_2, \quad (\text{B15})$$

with $\delta\lambda_1$ and $\delta\lambda_2$ determined from Eqs. (B10) and (B11).

Now

$$A = \Delta T + \frac{1}{2}\chi\Delta T^2, \quad (\text{B16})$$

and

$$\ln \frac{4\alpha t}{a^2 C} = \frac{A_1 - A_2}{G_1 - G_2}, \quad (\text{B17})$$

where $G = q/(4\pi\lambda)$. Thus, the error in thermal diffusivity, α , caused by a discrepancy in bath temperature δT_0 is

$$\begin{aligned} \frac{\delta\alpha}{\alpha} &= \frac{4\pi\lambda_0}{q_1 - q_2} \left(\delta T_{r1} + \chi\Delta t_1 \delta T_{r1} + \frac{1}{2} \Delta T_1^2 \delta\chi - \delta T_{r2} - \chi\Delta t_2 \delta T_{r2} - \frac{1}{2} \Delta T_2^2 \delta\chi \right) \\ &+ \frac{4\pi\delta\lambda_0}{q_1 - q_2} \left(\Delta T_1 + \frac{1}{2}\chi\Delta T_1^2 - \Delta T_2 - \frac{1}{2}\chi\Delta T_2^2 \right). \end{aligned} \quad (\text{B18})$$

Table BI. Calculated Temperature rise at Different Times as a Function of Power Before Correcting for the Influence of χ (Run ID's 1501 to 1508, Ref. 8)

q (W·m ⁻¹)	ΔT (K) @ 0.25 s	ΔT (K) @ 0.5 s	ΔT (K) @ 0.75 s	ΔT (K) @ 1.0 s
0.71525	3.79856	4.18564	4.41208	4.57273
0.65718	3.48267	3.83872	4.04699	4.19477
0.60151	3.18938	3.51425	3.70428	3.83911
0.54869	2.90400	3.20034	3.37369	3.49668
0.49287	2.63723	2.90573	3.06280	3.17424
0.45015	2.38302	2.62580	2.76782	2.86859
0.40460	2.14300	2.36079	2.48819	2.57859
0.77476	4.11724	4.53633	4.78149	4.95543

Table BII. Calculated Temperature rise at Different Times as a Function of Power After Correcting for the Influence of χ (Run ID's 1501 to 1508, Ref. 8)

G (K)	q (W·m ⁻¹)	A (K) @ 0.25 s	A (K) @ 0.5 s	A (K) @ 0.75 s	A (K) @ 1.0 s
0.5529	0.71525	3.78116	4.16430	4.38824	4.54705
0.5080	0.65718	3.46806	3.82077	4.02694	4.17316
0.4650	0.60151	3.17713	3.49920	3.68748	3.82101
0.4242	0.54869	2.89385	3.18787	3.35976	3.48167
0.3852	0.49287	2.62885	2.89545	3.05132	3.16186
0.3480	0.45015	2.37618	2.61741	2.75845	2.85849
0.3128	0.40460	2.13747	2.35401	2.48062	2.57042
0.5989	0.77476	4.09681	4.51126	4.75349	4.92526

Table BIII. Thermal Diffusivity Before and After Correction (Run ID's 1501–1508, Ref. 8)

Power (W·m ⁻¹)	$\alpha \times 10^8$ (m ² ·s ⁻¹) Perkins et al. [8] (DSTAT, %)	$\alpha_0 \times 10^8$ (m ² ·s ⁻¹) corrected for χ	$\alpha_0 \times 10^8$ (m ² ·s ⁻¹) corrected for both χ and temperature offset
0.71525	6.46 (0.4)	6.70	6.80
0.65718	6.32 (0.5)	6.63	6.73
0.60151	6.48 (0.4)	6.66	6.77
0.54869	6.40 (0.6)	6.59	6.72
0.49287	6.50 (0.6)	6.60	6.74
0.45015	6.47 (0.7)	6.63	6.79
0.40460	6.58 (0.7)	6.66	6.84
0.77476	6.51 (0.3)	6.70	6.79
Average	6.465±0.077(1.19/0.52)	6.646±0.0413(0.62)	6.772±0.0406(0.60)

Table BIV. Calculated Temperature Rise at Different Times as a Function of Power Before Correcting for the Influence of χ (Run ID's 1601 to 1608, Ref. 8)

q (W·m ⁻¹)	ΔT (K) @ 0.25 s	ΔT (K) @ 0.5 s	ΔT (K) @ 0.75 s	ΔT (K) @ 1.0 s
0.81341	4.48397	4.94358	5.21243	5.40318
0.75186	4.14317	4.56917	4.81837	4.99518
0.69337	3.82159	4.21377	4.44318	4.60595
0.63755	3.50730	3.86758	4.07832	4.22786
0.58387	3.21143	3.54147	3.73453	3.87151
0.53246	2.92430	3.22513	3.40111	3.52596
0.48350	2.65552	2.92791	3.08725	4.20030
0.43695	2.39831	2.64420	2.78803	2.89008

Table BV. Calculated Temperature Rise at Different Times as a Function of Power After Correcting for the Influence of χ (Run ID's 1601 to 1608, Ref. 8)

G (K)	q (W·m ⁻¹)	A (K) @ 0.25 s	A (K) @ 0.5 s	A (K) @ 0.75 s	A (K) @ 1.0 s
0.6584	0.81341	4.46366	4.91862	5.18454	5.37312
0.6086	0.75186	4.12583	4.54785	4.79454	4.96948
0.5613	0.69337	3.80684	4.19564	4.42291	4.58410
0.5161	0.63755	3.49488	3.85231	4.06126	4.20945
0.4726	0.58387	3.20101	3.52866	3.72022	3.85608
0.4310	0.53246	2.91567	3.21451	3.38923	3.51316
0.3914	0.48350	2.64841	2.91916	3.07747	3.18975
0.3537	0.43695	2.39251	2.63706	2.78005	2.88148

Table BVI. Thermal Diffusivity Before and after Correction (Run ID's 1601 to 1608, Ref. 8)

Power (W·m ⁻¹)	$\alpha \times 10^8$ (m ² ·s ⁻¹) Perkins et al. [8] (DSTAT, %)	$\alpha_0 \times 10^8$ (m ² ·s ⁻¹) corrected for χ	$\alpha_0 \times 10^8$ (m ² ·s ⁻¹) corrected for both χ and temperature offset
0.81341	6.21 (0.8)	6.30	6.43
0.75186	6.08 (0.3)	6.32	6.46
0.69337	6.16 (0.3)	6.33	6.49
0.63755	6.12 (0.4)	6.26	6.43
0.58387	6.10 (0.4)	6.27	6.46
0.53246	6.06 (0.5)	6.23	6.42
0.48350	6.18 (0.5)	6.23	6.45
0.43695	6.20 (0.6)	6.21	6.45
Average	6.139±0.057(0.93/0.48)	6.269±0.045(0.72)	6.449±0.022(0.34)

Table BVII. Uncertainty in the Determined Thermal Diffusivity Caused by the Uncertainty of Bath Temperature When Different Pairs of Points Are Used (Run ID's 1601 to 1608, Ref. 8)

Point pair	Power difference (W·m ⁻¹)	$\delta\alpha/\alpha \times 100$ (%)	Point pair	Power difference (W·m ⁻¹)	$\delta\alpha/\alpha \times 100$ (%)
1601 + 1602	0.06155	-0.60	1603 + 1605	0.10950	-0.04
1601 + 1603	0.12004	-0.62	1603 + 1606	0.16091	-0.19
1601 + 1604	0.17586	0.15	1603 + 1607	0.20987	0.25
1601 + 1605	0.22954	-0.34	1603 + 1608	0.25642	0.26
1601 + 1606	0.28095	-0.43	1604 + 1605	0.05368	1.18
1601 + 1607	0.32991	-0.06	1604 + 1606	0.10509	0.85
1601 + 1608	0.37376	-0.01	1604 + 1607	0.15405	-1.63
1602 + 1603	0.05849	-0.24	1604 + 1608	0.20060	-1.0
1602 + 1604	0.11431	0.59	1605 + 1606	0.05141	-0.26
1602 + 1605	0.16799	-0.11	1605 + 1607	0.10037	-0.14
1602 + 1606	0.21940	-0.20	1605 + 1608	0.14692	-0.32
1602 + 1607	0.26836	0.13	1606 + 1607	0.04896	0.53
1602 + 1608	0.31491	0.15	1606 + 1608	0.09551	0.55
1603 + 1604	0.05582	1.57	1607 + 1608	0.04655	0.31

To examine the possible magnitude of this on experimental thermal diffusivity data the measurements of Perkins et al. [8] at 422 K (Run ID 1601 to 1608) will be taken as an example. The mean temperature for the eight measurements is 422.510 ± 0.047 K ($\pm 0.011\%$: max: +72 and 51 mK (+0.017 and -0.012%)). If measurement pairs of the complete data set are used, the results are listed in Table BVII. The use of any pair of points to obtain a thermal diffusivity value at the mean bath temperature results in a maximum error of about 1.6%. If all the points are used to determine the thermal diffusivity the standard deviation is 0.51% (RMS = 0.502%). It can be expected, therefore, that if all the data points are employed in the linear regression of A ~ G to obtain thermal diffusivity, the resulting uncertainty caused by a bath temperature disturbance of say ± 47 mK will be less than $\pm 0.5\%$. This uncertainty is of the same order as that resulting for the thermal diffusivity itself, i.e., a value of DSTAT = 0.3 to 0.6%.

ACKNOWLEDGMENT

This work was performed under a program of studies funded by the Natural Sciences and Engineering Research Council of Canada, under NSERC OPG 8859.

REFERENCES

1. Y. Nagasaka and A. Nagashima, *J. Phys. E* **14**:1425 (1981).
2. L. Sun, J. E. S. Venart, and R. C. Prasad, *Int. J. Thermophys.* (in press).
3. Sun, L., Ph.D. Thesis (The University of New Brunswick, Canada, in press).
4. L. Sun, J. E. S. Venart, and R. C. Prasad, *Int. J. Thermophys.* (in press).
5. J. J. Healy, J. J. de Groot, and J. Kestin, *Physica* **82C**:392 (1976).
6. J. Menashe and W. A. Wakeham, *Int. J. Heat Mass Transfer* **25**:661 (1982).
7. C. A. Nieto de Castro, S. F. Y. Li, G. C. Maitland, and W. A. Wakeham, *Int. J. Thermophys.* **4**:311 (1983).
8. R. A. Perkins, H. M. Roder, and C. A. Nieto de Castro, *J. Res. Natl. Inst. Stand. Technol.* **96**:247 (1991).
9. C. A. Nieto de Castro, R. A. Perkins, and H. M. Roder, *Int. J. Thermophys.* **12**:985 (1991).
10. National Institute of Standards and Technology, Standard Reference Database 14, Mixture Property Database (NIST14), Version 9.09 (1993)
11. National Institute of Standards and Technology, Standard Reference Database 4, NIST Thermophysical Properties of Hydrocarbon Mixtures Program, SUPERTRAPP-Version 1.07 (1990).
12. G. H. Wang, J. E. S. Venart, and R. C. Prasad, *Proc. 11th Symp. on Thermophys. Props.*, June 23–27, Boulder, Colorado, U.S.A. (1991).
13. M. L. V. Ramires, F. J. Viera dos Santos, U. V. Mardolcar, and C. A. Nieto de Castro, *Int. J. Thermophys.* **10**:1005 (1989).
14. N. Mani and J. E. S. Venart, *Proc. 6th Symp. Thermophys. Prop.*, P. E. Liley, ed. (ASME, New York, 1974), p. 1.
15. V. M. Shulga, F. G. Eldarov, Y. U Atanov, and A. A. Kuyumchev, *Int. J. Thermophys.* **7**:1147 (1986).
16. R. A. Perkins, M. L. V. Ramires, and C. A. Nieto de Castro, *J. Res. Natl. Inst. Stand. Technol.* **105**:255 (2000).
17. S. Will, A. P. Froba, and A. Leipertz, *Int. J. Thermophys.* **19**: 403 (1998).
18. H. S. Carslaw and J. G. Jaeger, *Conduction of Heat in Solids*, 2nd Ed. (Clarendon Press, Oxford, 1959).